

# Unveiling traces of primordial non-Gaussianity in the cosmic web with *WebSky*

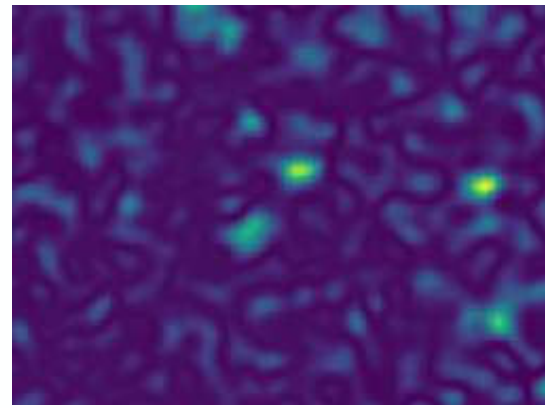
**Nathan J. Carlson (PhD candidate, CITA / University of Toronto)**

J. Richard Bond, Jonathan Braden, Dongwoo T. Chung, Patrick Horlville, Zack Li, Thomas Morrison

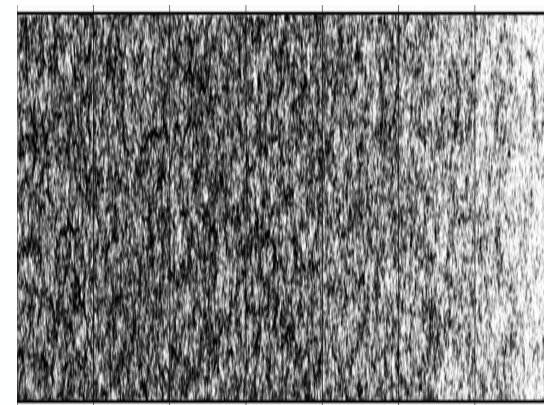
**Cosmology From Home - Jul 2023**



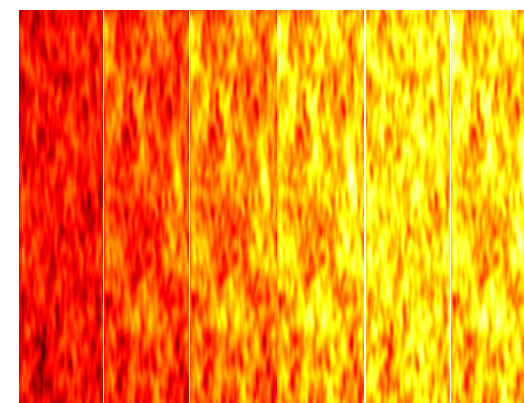
# In this talk I'll discuss how we can look for signatures of novel early-universe physics in the Cosmic Web



**What is non-Gaussianity  
and how do we measure it?**



**The *Peak-Patch/WebSky2.0* Pipeline**  
for fast generation of mock cosmological observables



**Constraining inflation**  
with statistics of mock sky maps

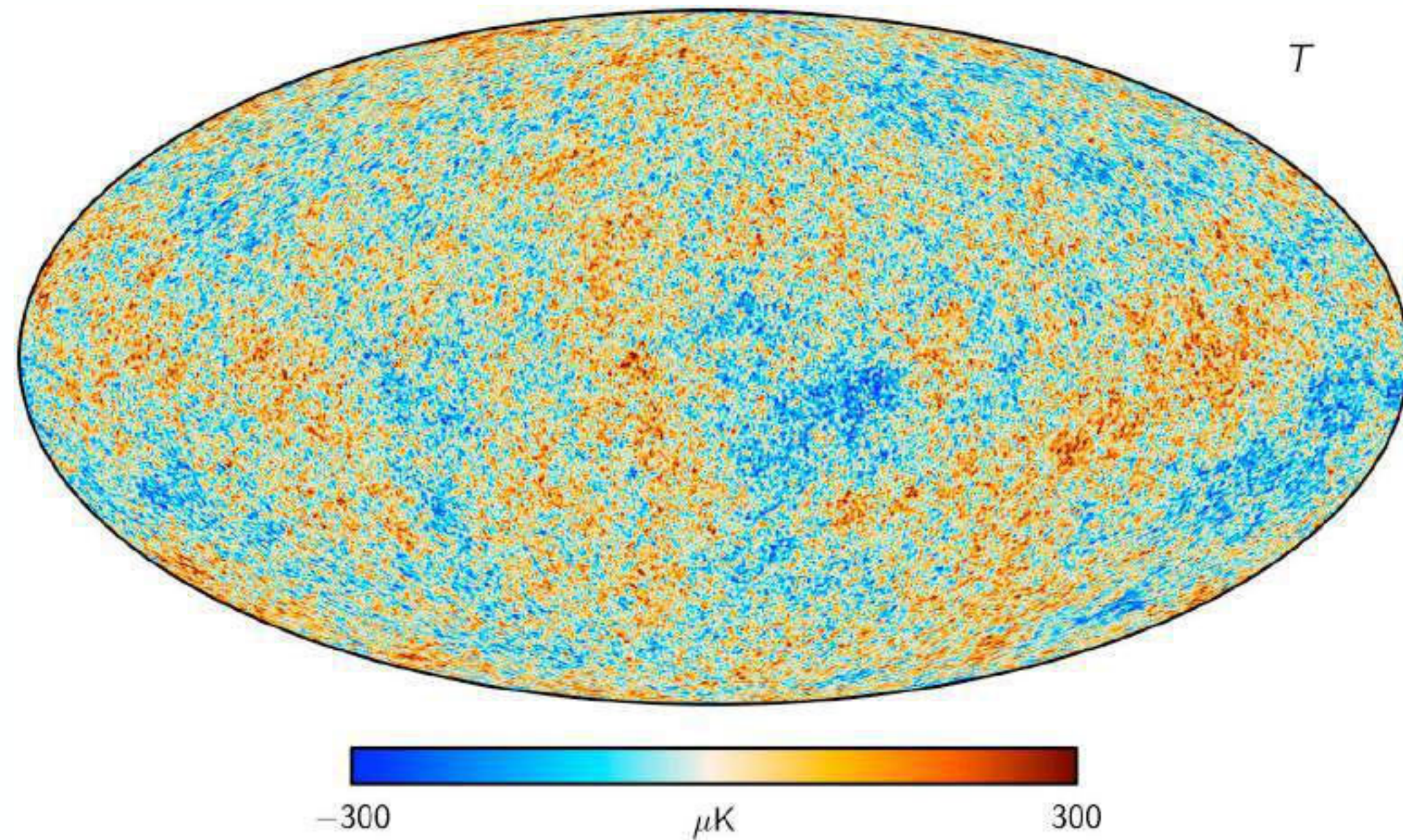
We will soon be putting out a new public release of WebSky catalogues with a range of non-Gaussian initial conditions.



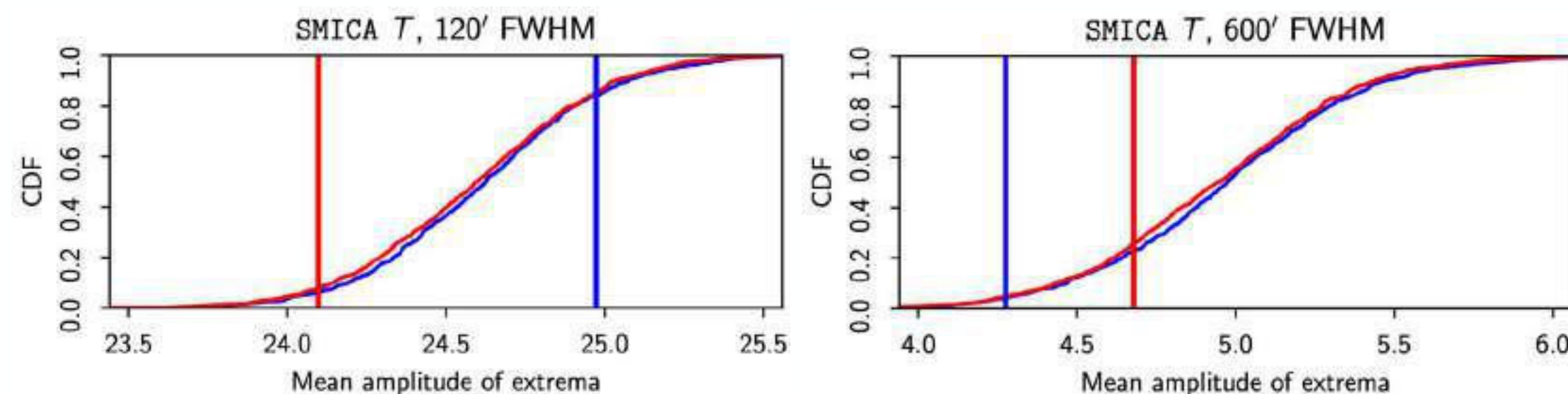
# What is non-Gaussianity and how do we measure it?



**The CMB demonstrates that the distribution of energy in the early universe was very nearly Gaussian, but all inflation models predict some deviation from purely Gaussian statistics.**



SMICA CMB temperature map (above) [1807.06208] and extrema CDFs (below) [1906.02552v2] from *Planck* Collaboration's 2018 results showing that the CMB is highly Gaussian.



Characterizing the deviation from purely Gaussian statistics (the “non-Gaussianity”) allows us to constrain the parameter space of inflation.

Other physics introduce non-Gaussianities (e.g. nonlinear processes like gravitational collapse). We need to be able to distinguish between early universe non-Gaussianity and the foregrounds of late-time physics to extract inflationary signatures.

**So how can we characterize the non-Gaussianity of the very early universe?**

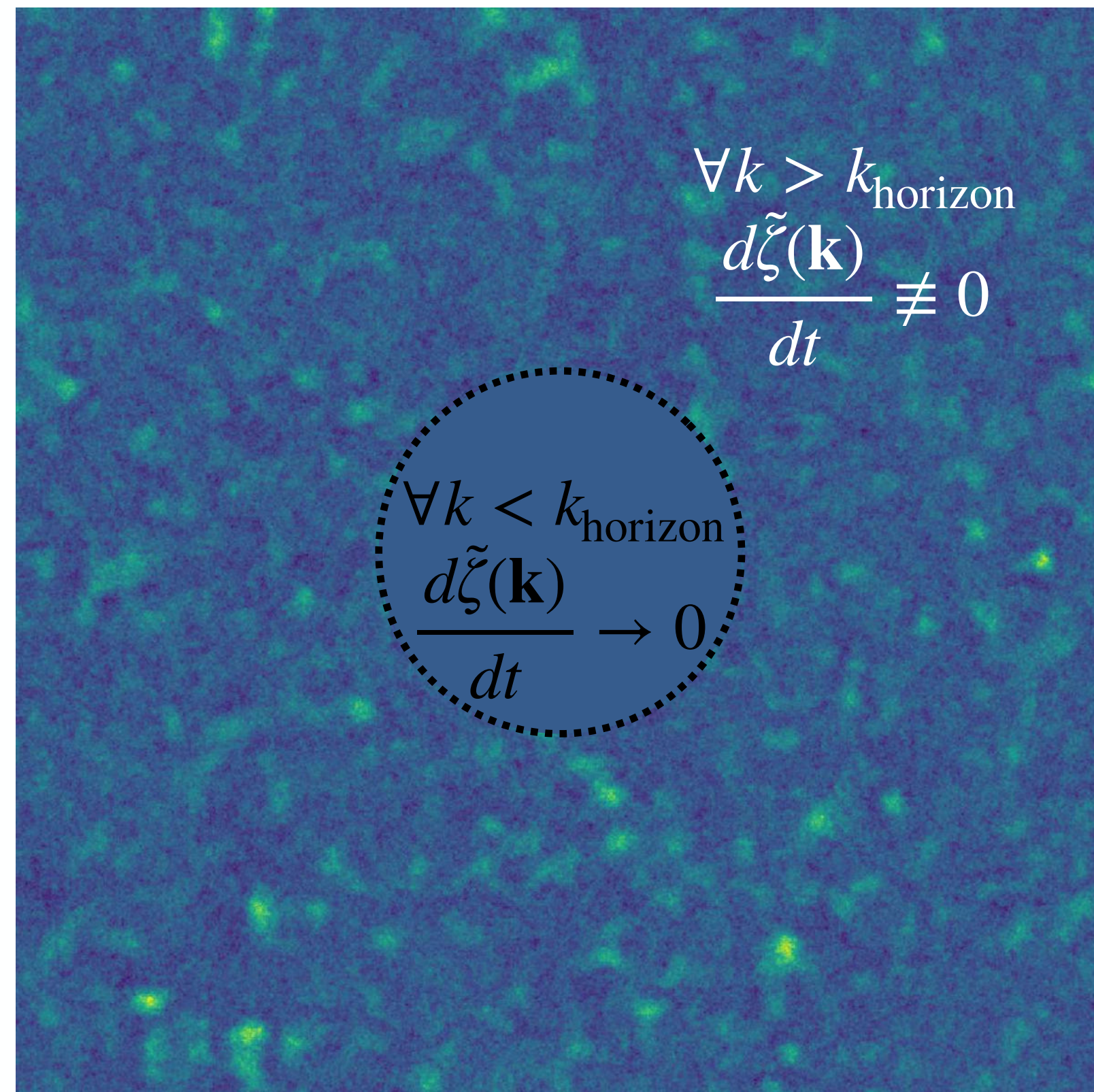
**And how can we isolate primordial non-Gaussianity from foregrounds?**



**So how can we characterize the non-Gaussianity of the very early universe?**



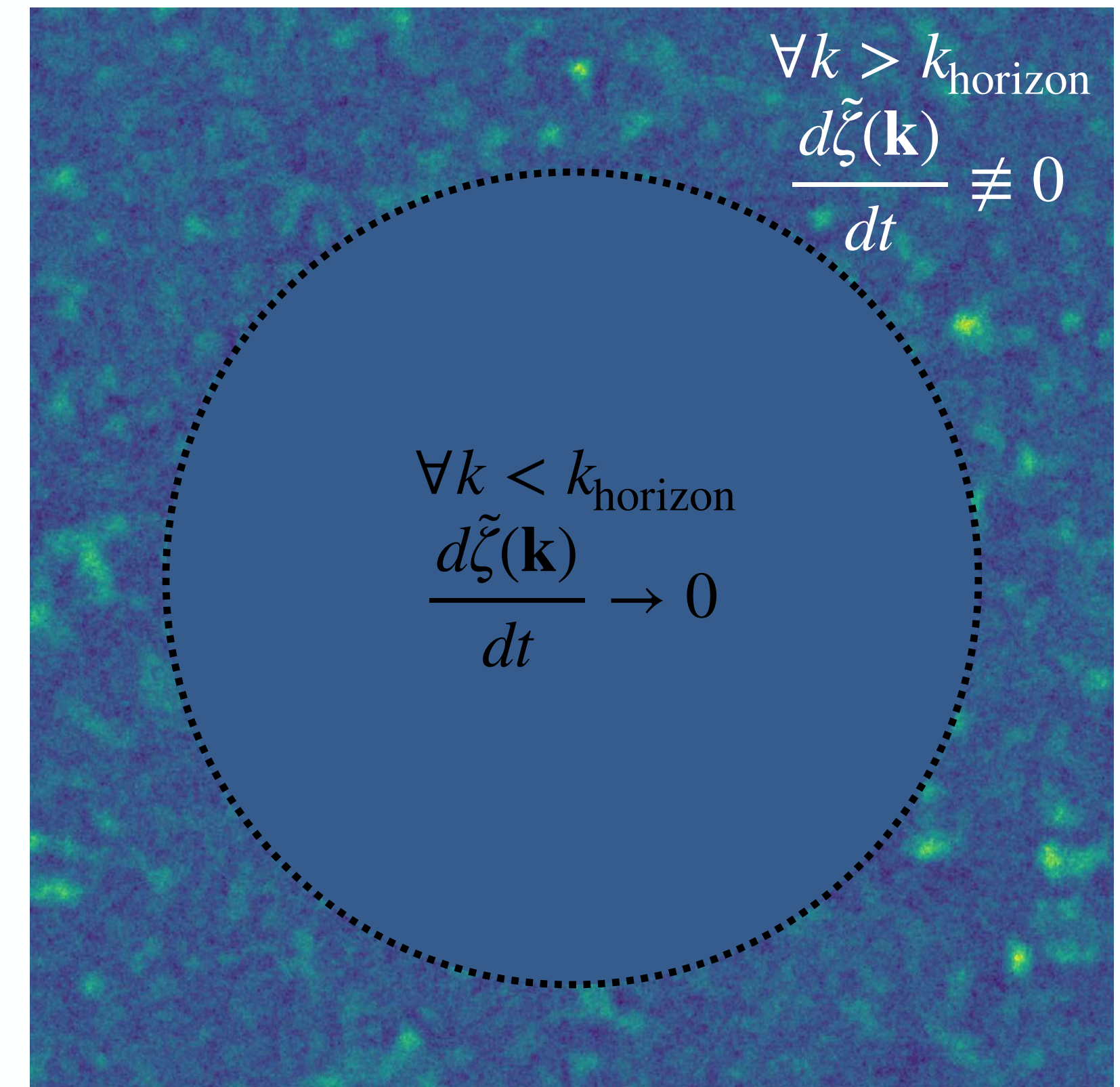
$\zeta$  is an early universe scalar perturbation field that couples to observables like the energy density of the universe  $\delta$ . It has the useful feature that it stops evolving on super-horizon scales.



During inflation,  $k$  modes are transported across the horizon as  $k_{\text{horizon}}$  increases.



This causes  $\tilde{\zeta}(\mathbf{k})$  to stop evolving with time so a larger  $k$ -space volume freezes out as inflation proceeds.



As  $\zeta$  modes freeze out, they preserve information from the corresponding time during inflation. As the horizon expands again post-inflation, modes re-enter and begin to evolve, interacting with other, observable fields, allowing us to probe the inflationary epoch.



**The lowest-order non-Gaussian term that can arise from single-field inflation is from a quadratic coupling to a single underlying Gaussian field. This is tightly constrained by bispectrum.**

$$\zeta(\mathbf{x}) = \zeta_G(\mathbf{x}) + f_{\text{NL}} \left( \zeta_G^2(\mathbf{x}) - \langle \zeta_G^2(\mathbf{x}) \rangle \right)$$

Gaussian  
component

Amplitude  
(sort of...)

Non-Gaussian component is a  
function of Gaussian component

CMB bispectra constrain this form of non-Gaussianity to  $f_{\text{NL}}^{\text{local}} = -0.9 \pm 5.1$ ,  $f_{\text{NL}}^{\text{equil}} = -26 \pm 47$ ,  $f_{\text{NL}}^{\text{ortho}} = -38 \pm 24$  with 1- $\sigma$  C.L. [1905.05697].  $|\zeta| \lesssim 10^{-5}$ , so these are strong constraints.



**The lowest-order non-Gaussian term that can arise from single-field inflation is from a quadratic coupling to a single underlying Gaussian field. This is tightly constrained by bispectrum.**

$$\zeta(\mathbf{x}) = \zeta_G(\mathbf{x}) + f_{\text{NL}} \left( \zeta_G^2(\mathbf{x}) - \langle \zeta_G^2(\mathbf{x}) \rangle \right)$$

Gaussian component

$$\begin{aligned} \zeta(\mathbf{x}) &= \zeta_G(\mathbf{x}) + f_{\text{NL}} \left( \zeta_G^2(\mathbf{x}) - \sigma_{\zeta_G}^2 \right) \\ &= \zeta_G(\mathbf{x}) + \bar{f}_{\text{NL}} \left( \frac{\zeta_G^2(\mathbf{x})}{\sigma_{\zeta_G}^2} - 1 \right) \end{aligned}$$

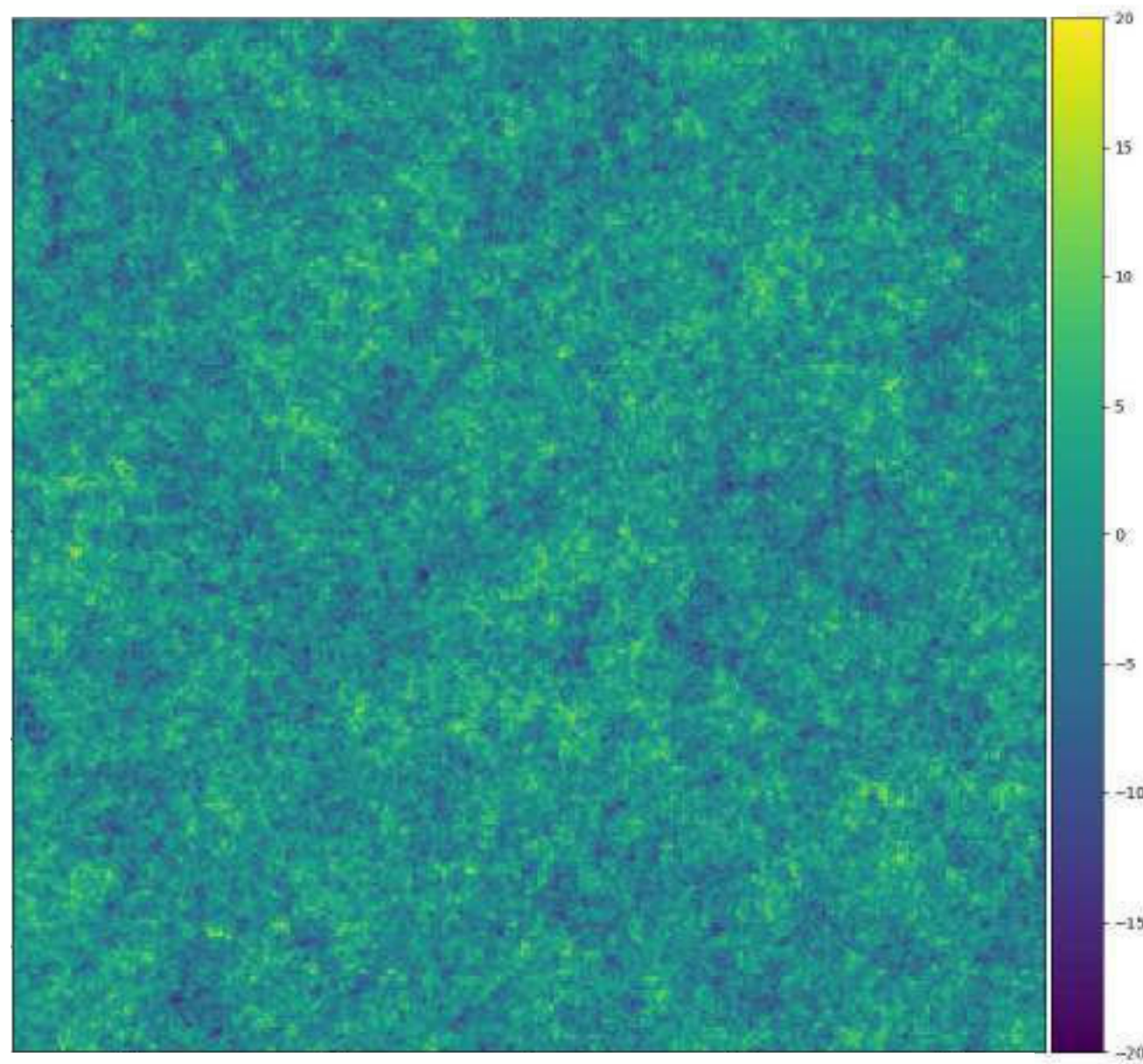
Non-Gaussian component is a function of Gaussian component

CMB bispectra constrain this form of non-Gaussianity to  $f_{\text{NL}}^{\text{local}} = -0.9 \pm 5.1$ ,  $f_{\text{NL}}^{\text{equil}} = -26 \pm 47$ ,  $f_{\text{NL}}^{\text{ortho}} = -38 \pm 24$  with 1- $\sigma$  C.L. [1905.05697].  $|\zeta| \lesssim 10^{-5}$ , so these are strong constraints.



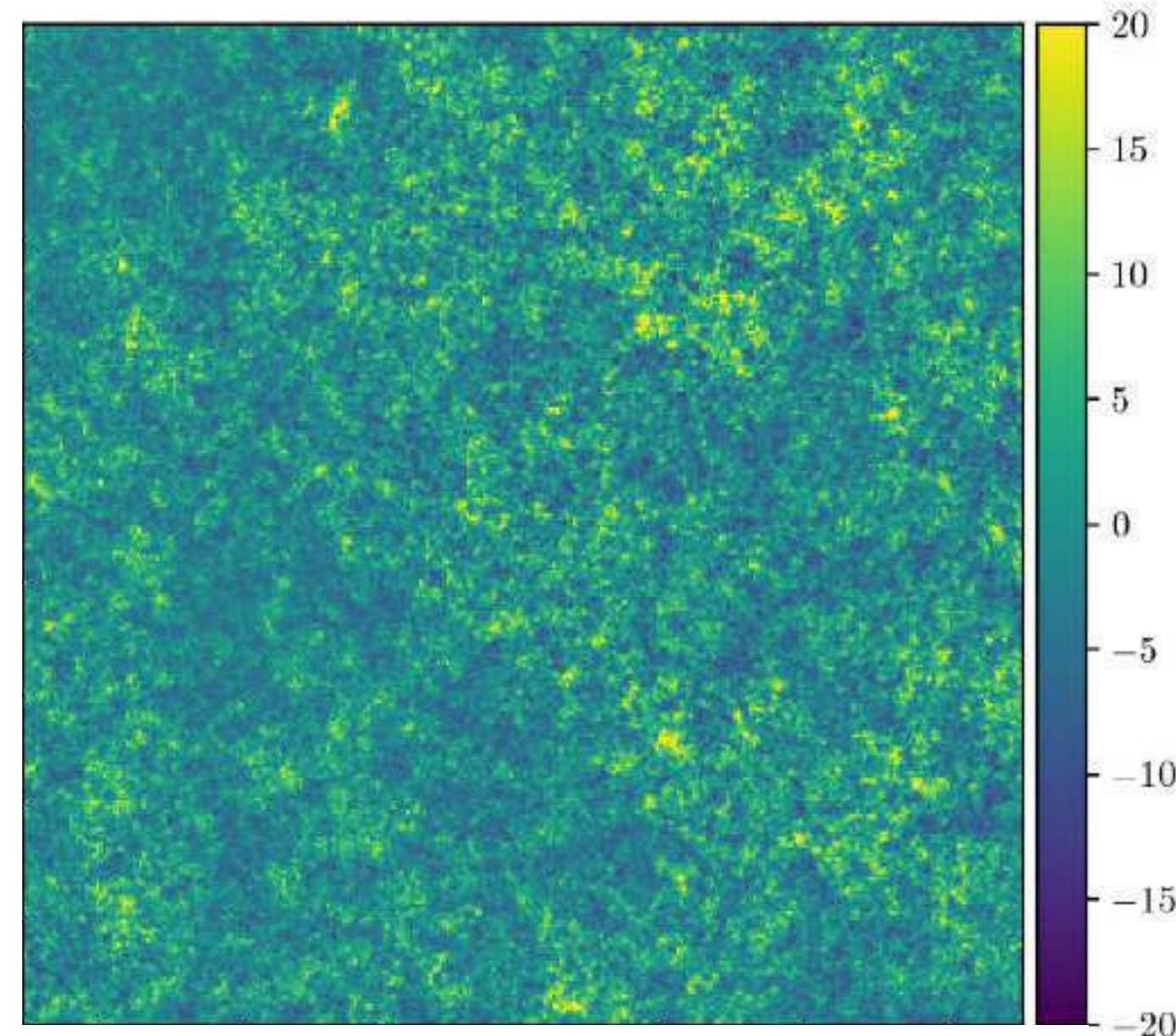
**There are other mechanisms that can generate non-Gaussianity that is not correlated to the underlying Gaussian field. In such cases, similar “ $f_{\text{NL}}$ ” give considerably less effect.**

Gaussian overdensity  $\delta_G(\mathbf{x})$



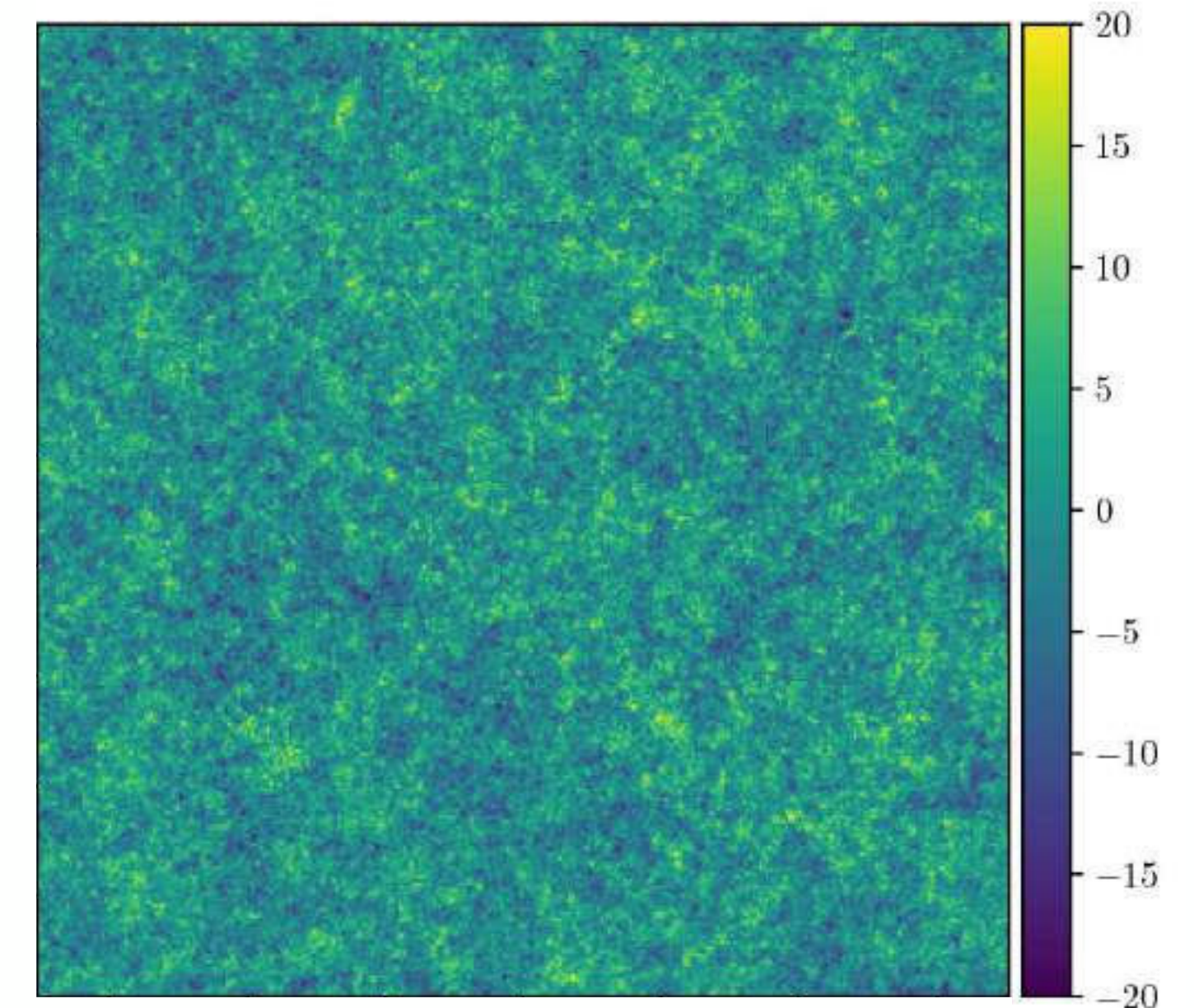
Underlying Gaussian sourced only by  $\zeta_G(\mathbf{x})$

non-Gaussian  $\delta_{nG}(\mathbf{x})$  **correlated** with  $\delta_G(\mathbf{x})$



Classical  $f_{\text{NL}}$  non-Gaussianity sourced by  $\zeta(\mathbf{x}) = \zeta_G(\mathbf{x}) + f_{\text{NL}} (\zeta_G^2(\mathbf{x}) - \langle \zeta_G^2(\mathbf{x}) \rangle)$  with  $f_{\text{NL}} = 10^5$ .

non-Gaussian  $\delta_{nG}(\mathbf{x})$  **uncorrelated** with  $\delta_G(\mathbf{x})$

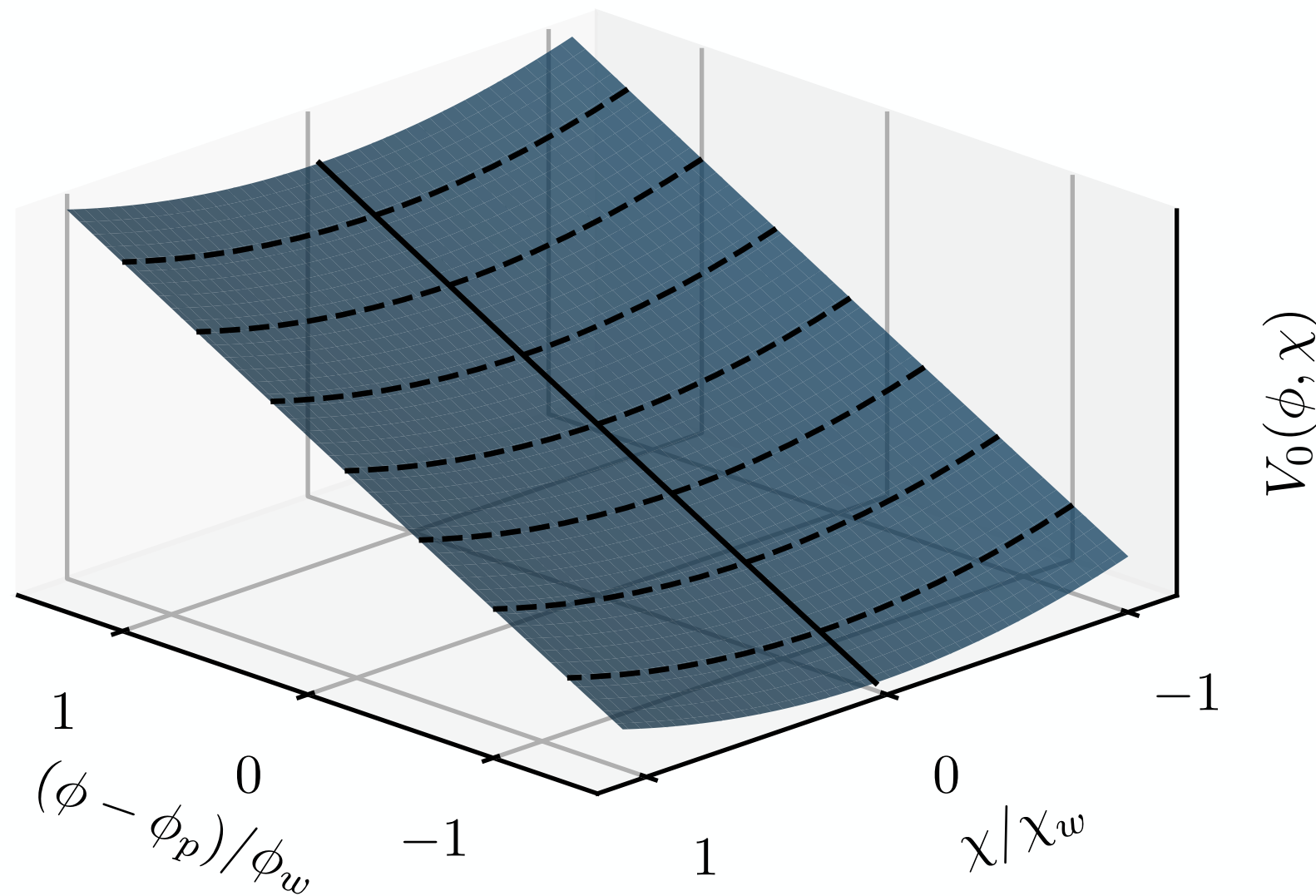


Uncorrelated gaussian field  $\chi_G(\mathbf{x})$  with nearly scale-invariant power spectrum giving rise to non-Gaussianity sourced by  $\zeta(\mathbf{x}) = \zeta_G(\mathbf{x}) + \tilde{f}_{\text{NL}} (\chi_G^2(\mathbf{x}) - \langle \chi_G^2(\mathbf{x}) \rangle)$  with  $\tilde{f}_{\text{NL}} = 10^5$

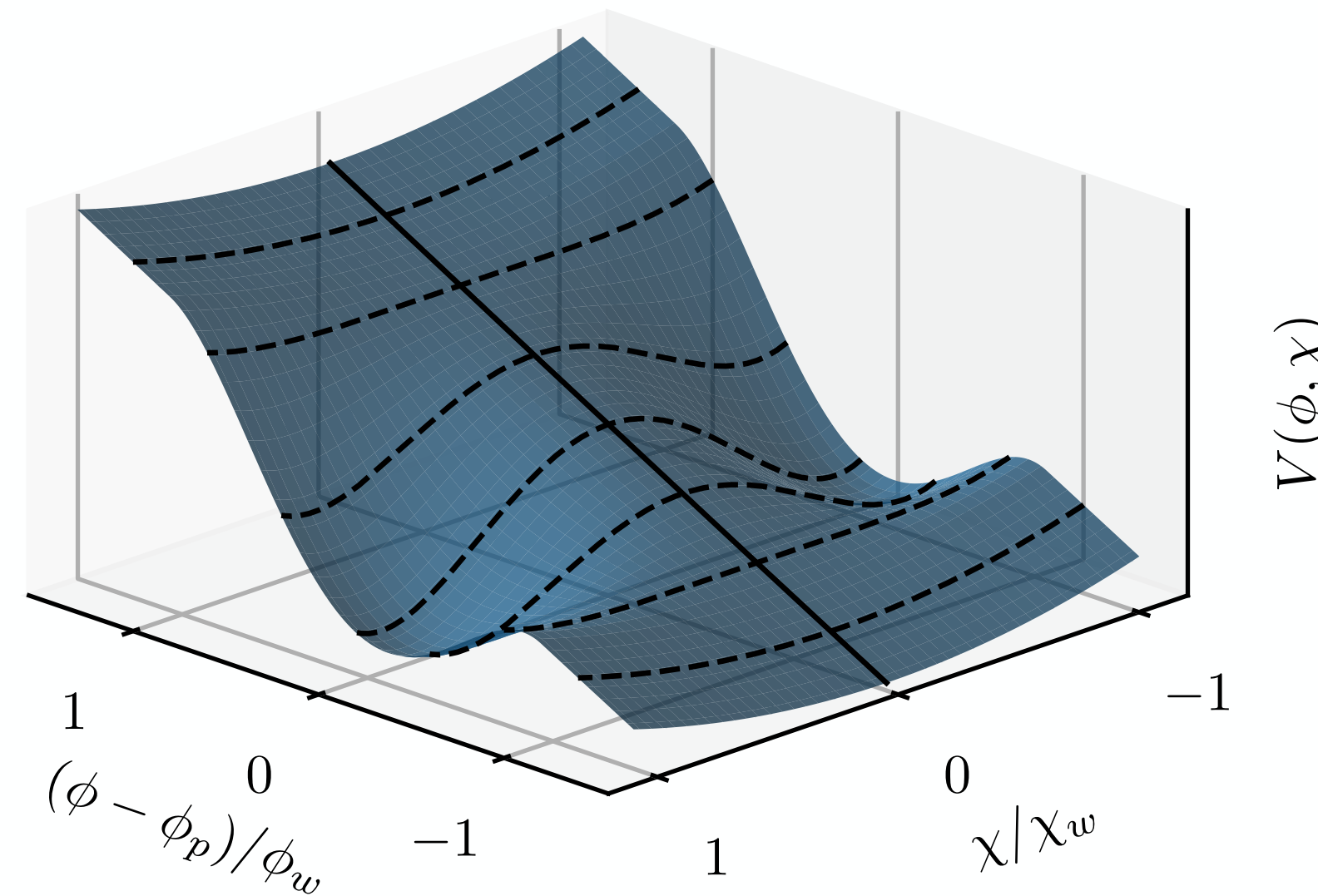


# Instabilities in the inflationary potential produce **primordial intermittent non-Gaussianities (PINGs)** that are uncorrelated and form isolated peaks at a characteristic scale. The bispectrum is particularly insensitive to this.

Background potential (before and after instability) featuring no saddle points.



Potential during instability featuring saddle points.



A simple example is the above potential which exhibits a saddle point when the inflaton is in the instability regime  $\phi \in (\phi_p - \phi_w, \phi_p + \phi_w)$ . The potential surface is described by

$$V(\phi, \chi) = \begin{cases} V_0(\phi, \chi) + \frac{\lambda_\chi}{4} \left[ \left( \frac{\phi - \phi_p}{\phi_w} \right)^2 - 1 \right]^2 \left[ (\chi^2 - v^2)^2 - v^4 \right] & \forall \phi \in (\phi_p - \phi_w, \phi_p + \phi_w) \\ V_0(\phi, \chi) & \forall \phi \notin (\phi_p - \phi_w, \phi_p + \phi_w) \end{cases}$$

where the background potential (*i.e.* the potential before and after the instability)  $V_0(\phi, \chi) = \frac{1}{2} m_\phi^2 \phi^2 + \frac{1}{2} m_\chi^2 \chi^2$

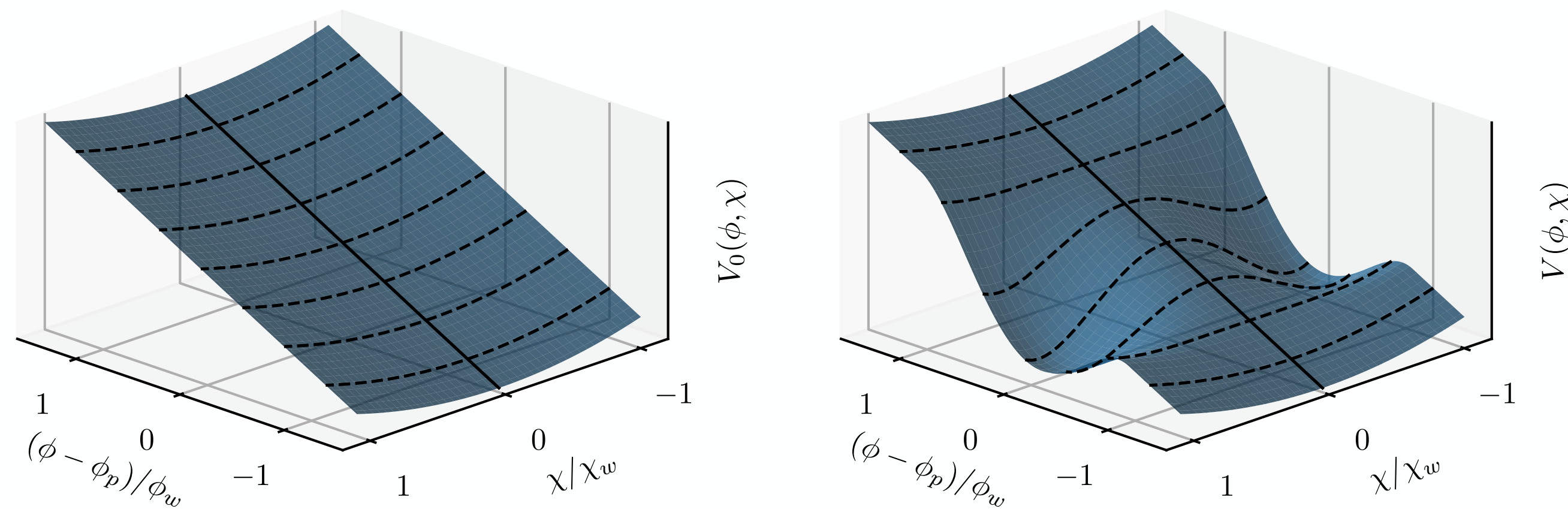
The transverse inflationary field  $\chi$  couples nonlinearly to  $\zeta$ , resulting in a non-Gaussian component of  $\zeta$  described by a **functional**

$$\zeta(\mathbf{x}) = \zeta_G(\mathbf{x}) + F_{\text{NL}} [\chi_G(\mathbf{x})]$$

I'm a functional, not a constant



Instabilities in the inflationary potential produce **primordial intermittent non-Gaussianities (PINGs)** that are uncorrelated and form isolated peaks at a characteristic scale. The bispectrum is particularly insensitive to this.

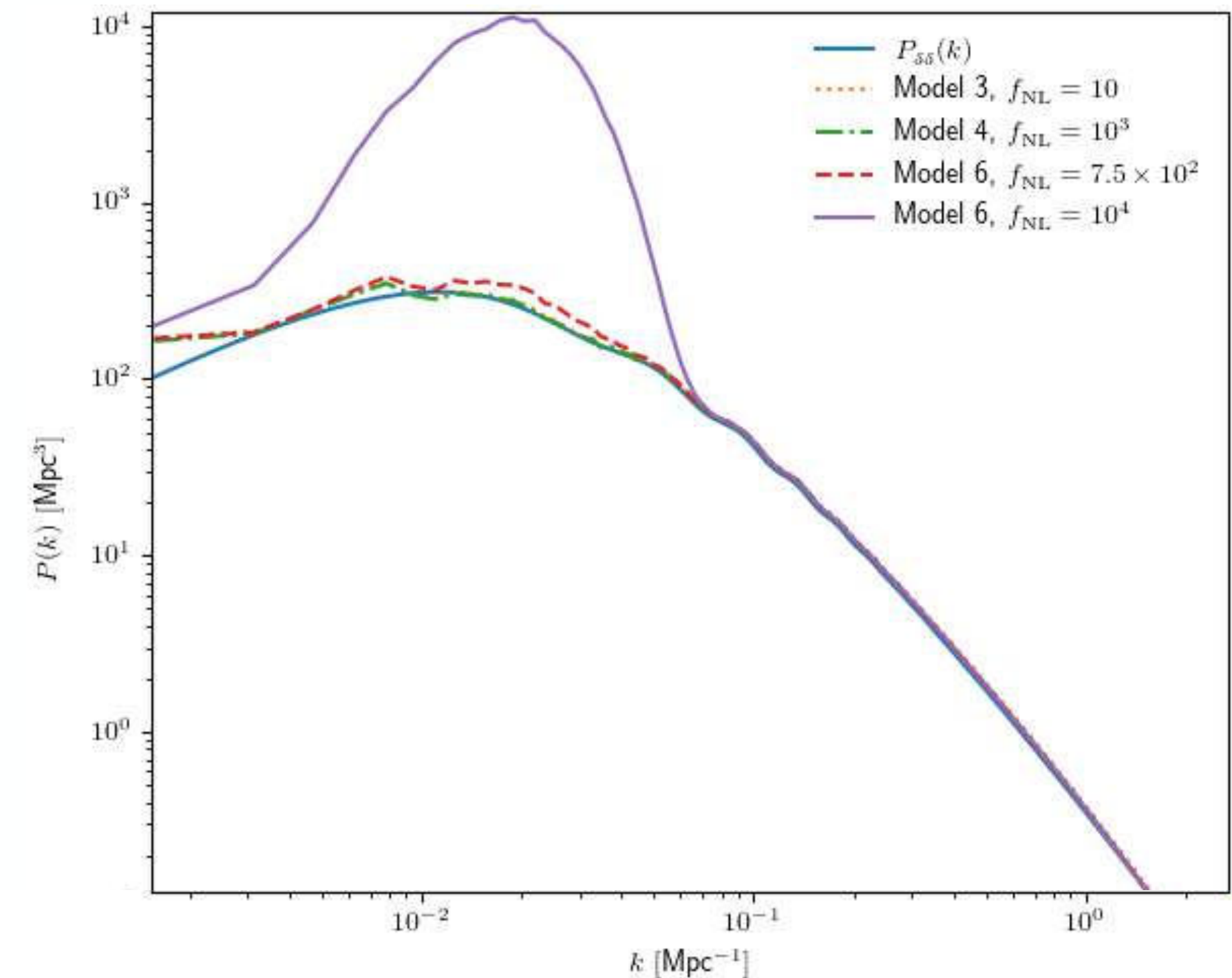


Results from lattice sims (**Morrison et al. 2023, in prep.**) give a power spectrum. I use these to model the Cosmic Web.

This potential feature results in non-Gaussianity with a **functional** form

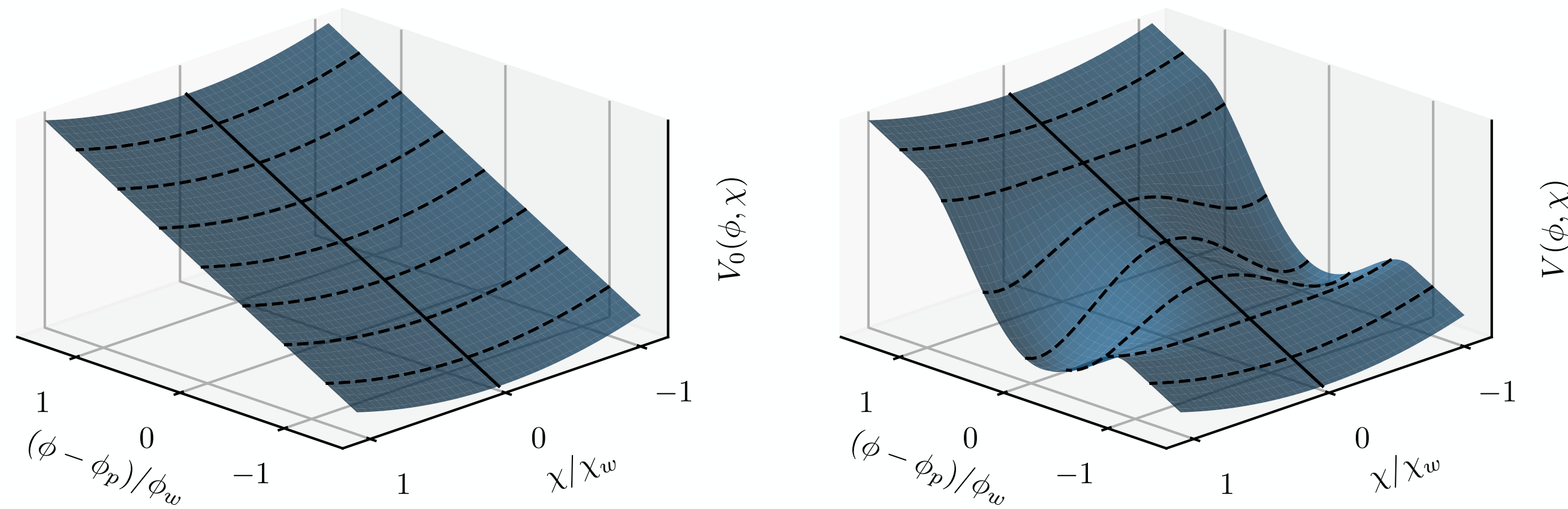
$$\zeta(\mathbf{x}) = \zeta_G(\mathbf{x}) + F_{\text{NL}} [\chi_G(\mathbf{x})]$$

I'm a functional,  
not a constant





Instabilities in the inflationary potential produce **primordial intermittent non-Gaussianities (PINGs)** that are uncorrelated and form isolated peaks at a characteristic scale. The bispectrum is particularly insensitive to this.

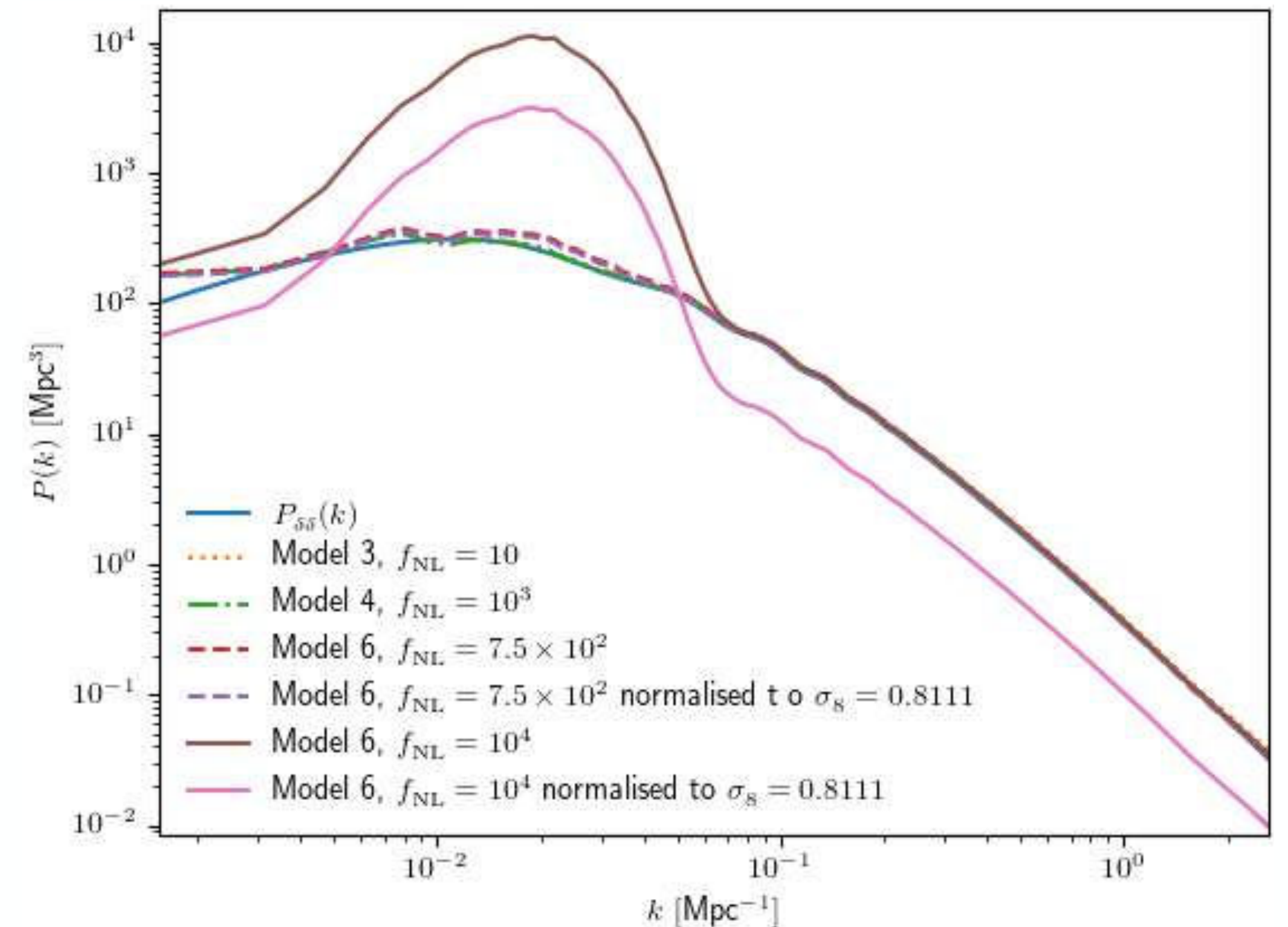


Results from lattice sims (**Morrison et al. 2023, in prep.**) give a power spectrum. I use these to model the Cosmic Web.

This potential feature results in non-Gaussianity with a **functional** form

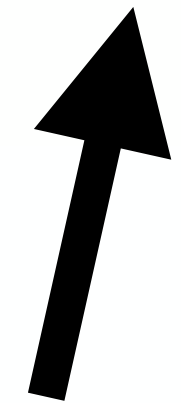
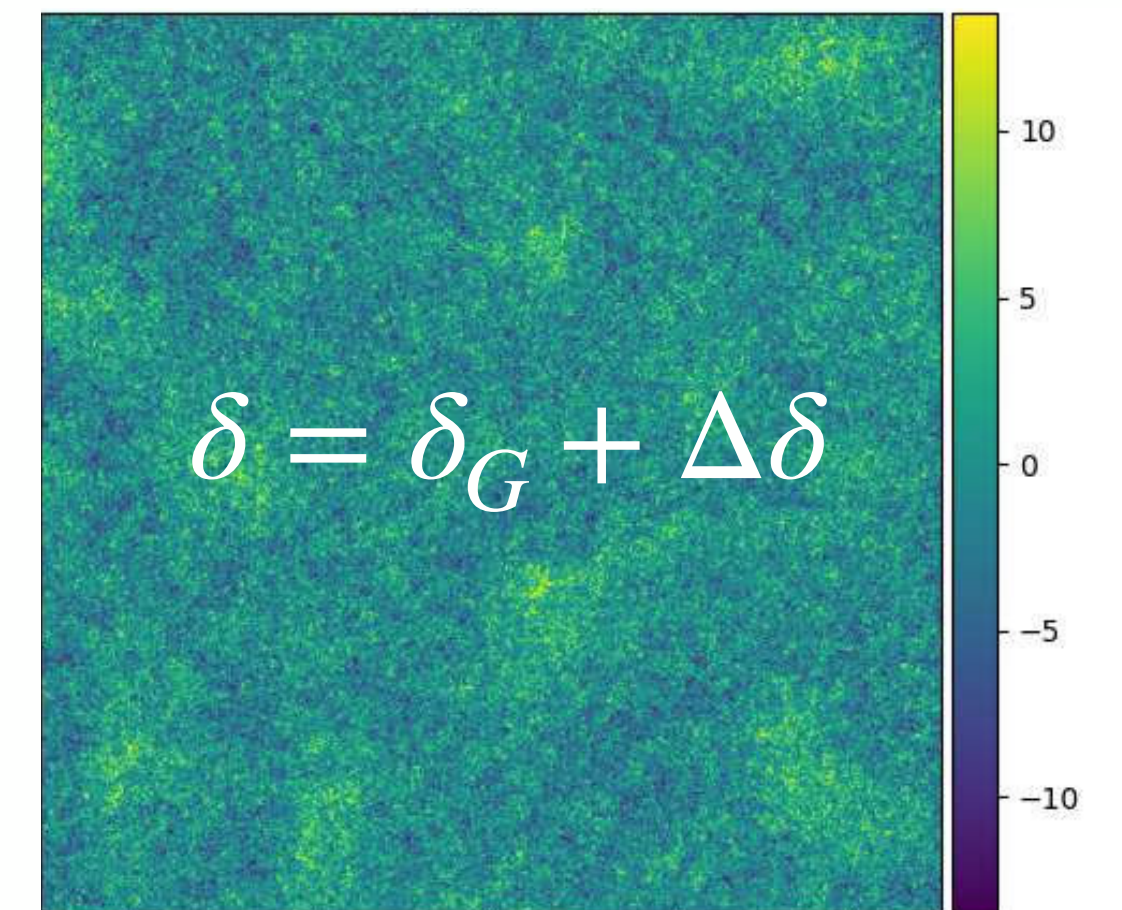
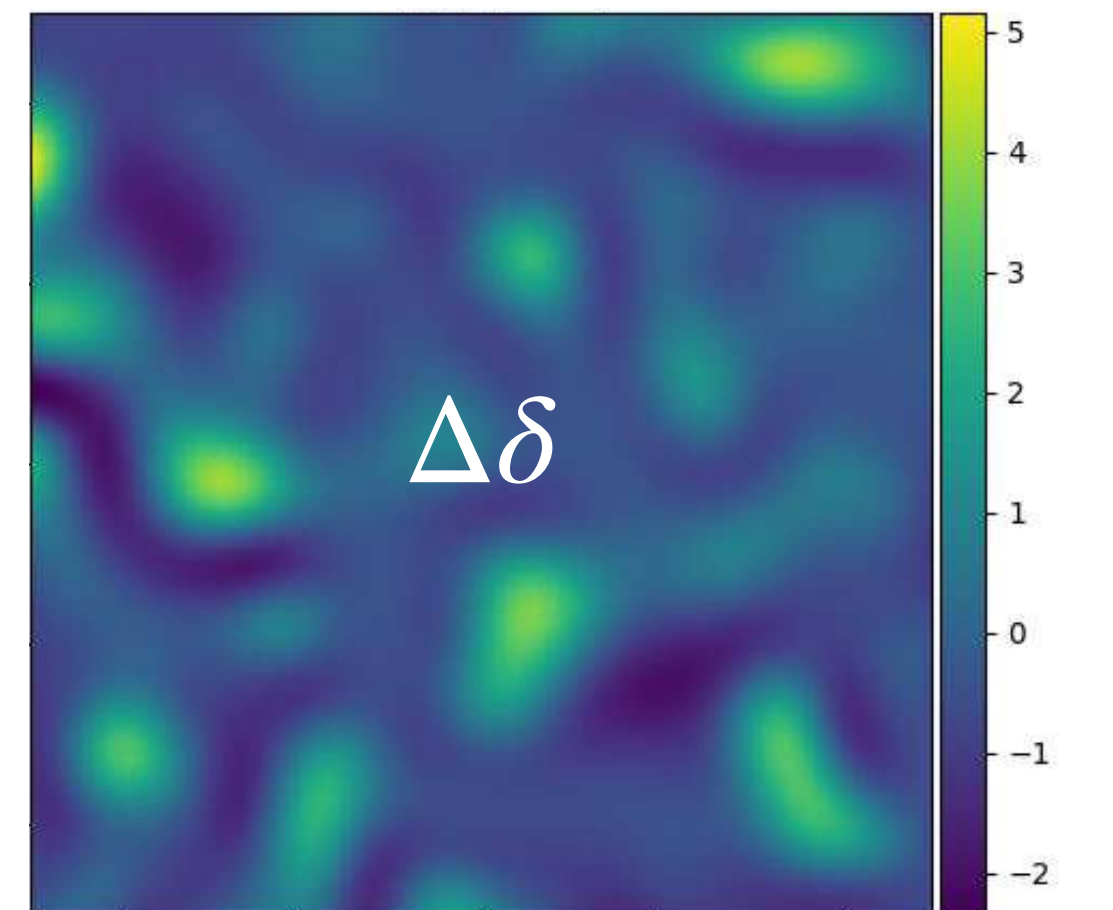
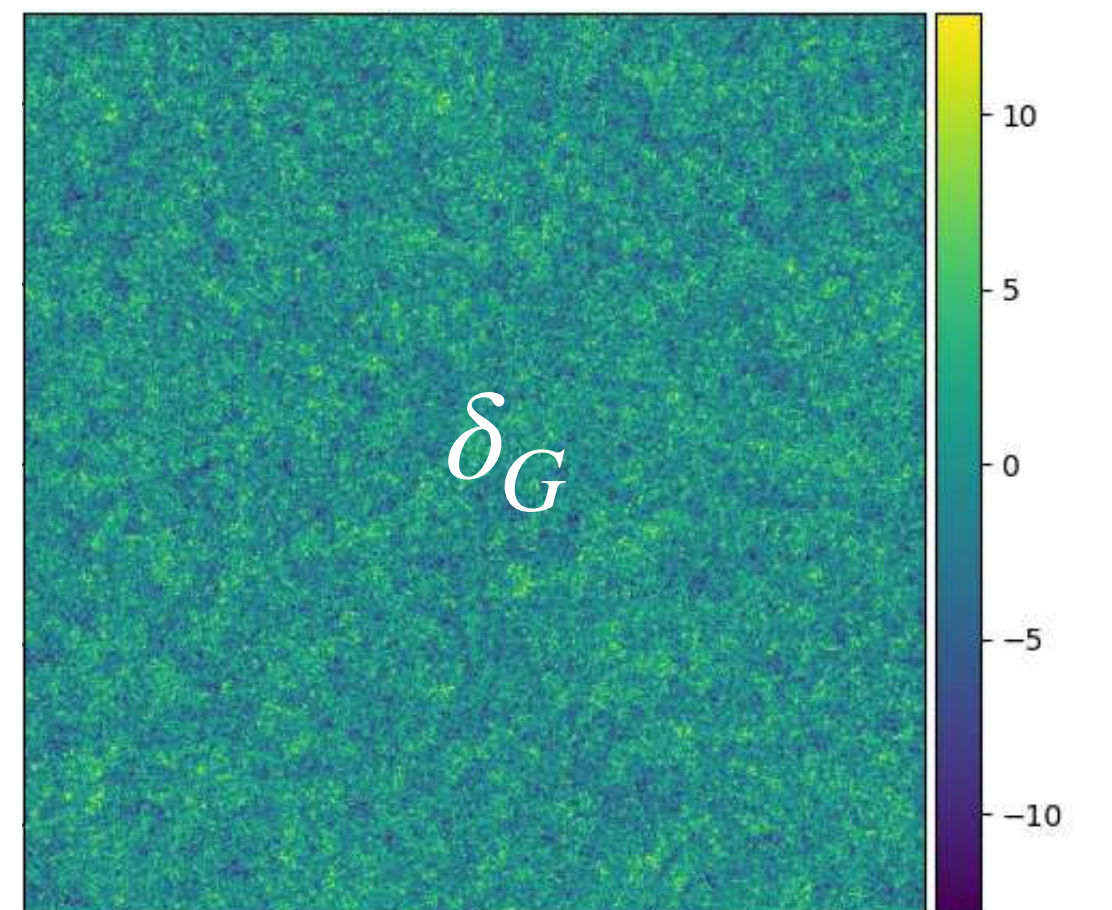
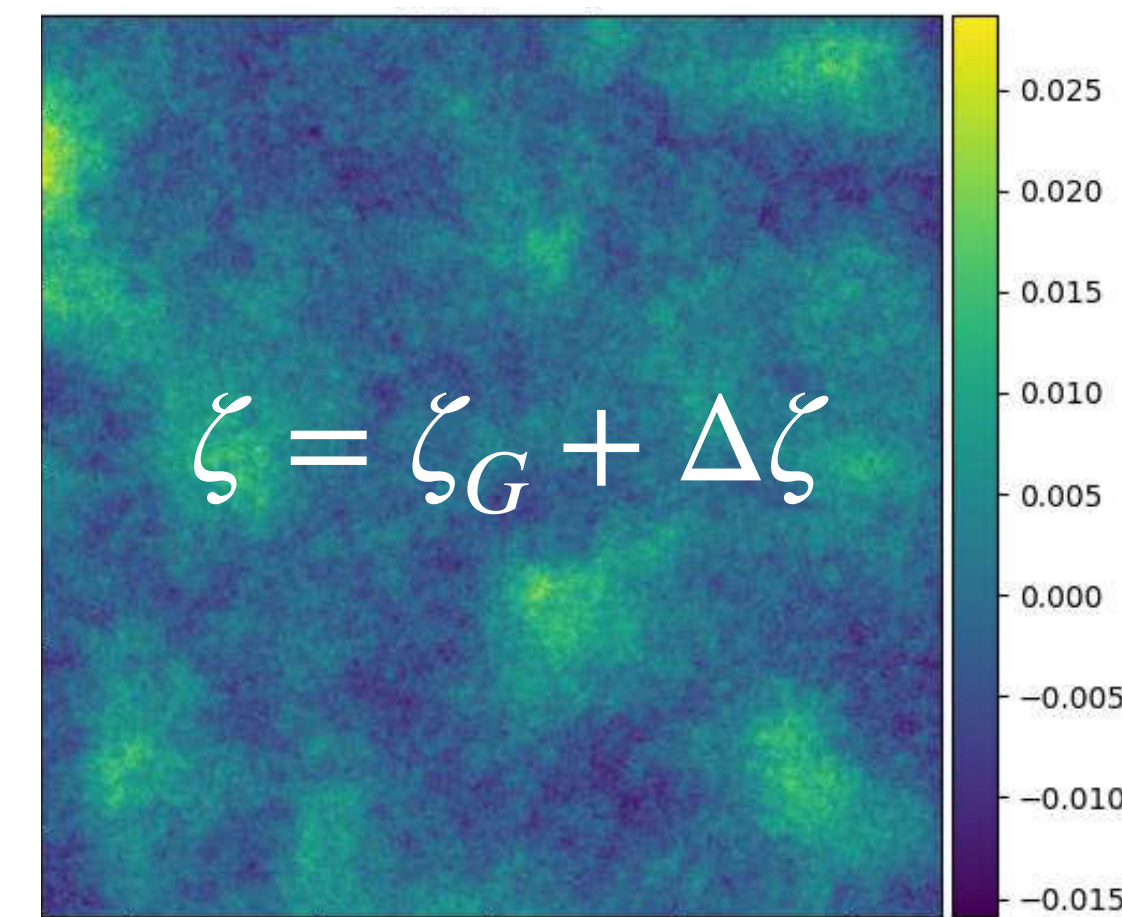
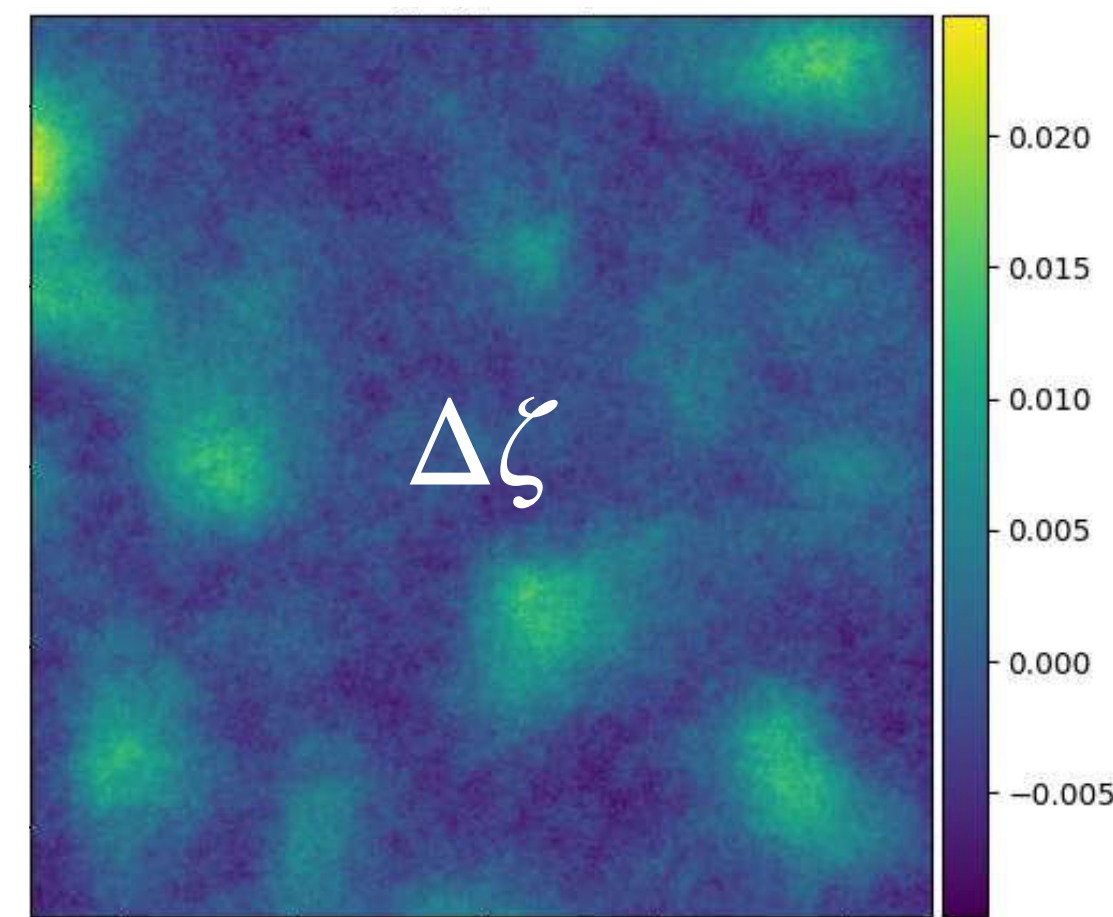
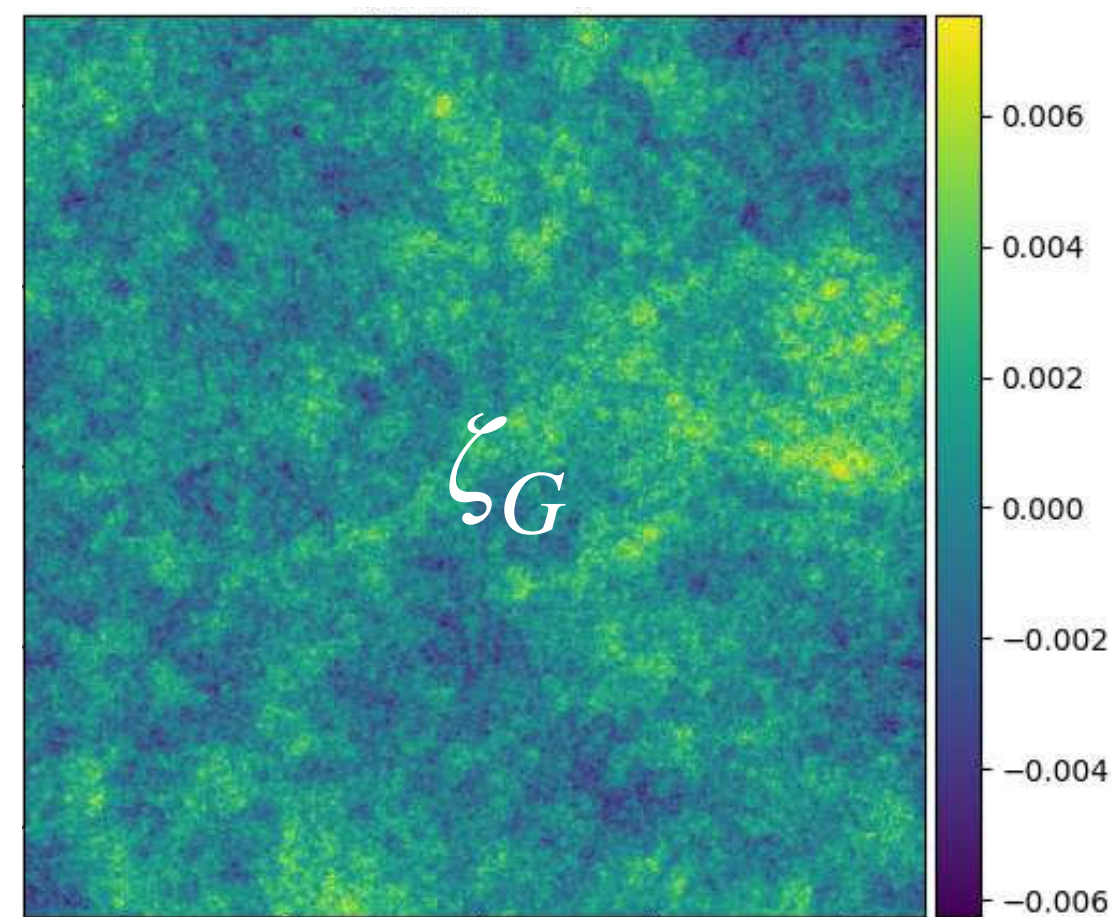
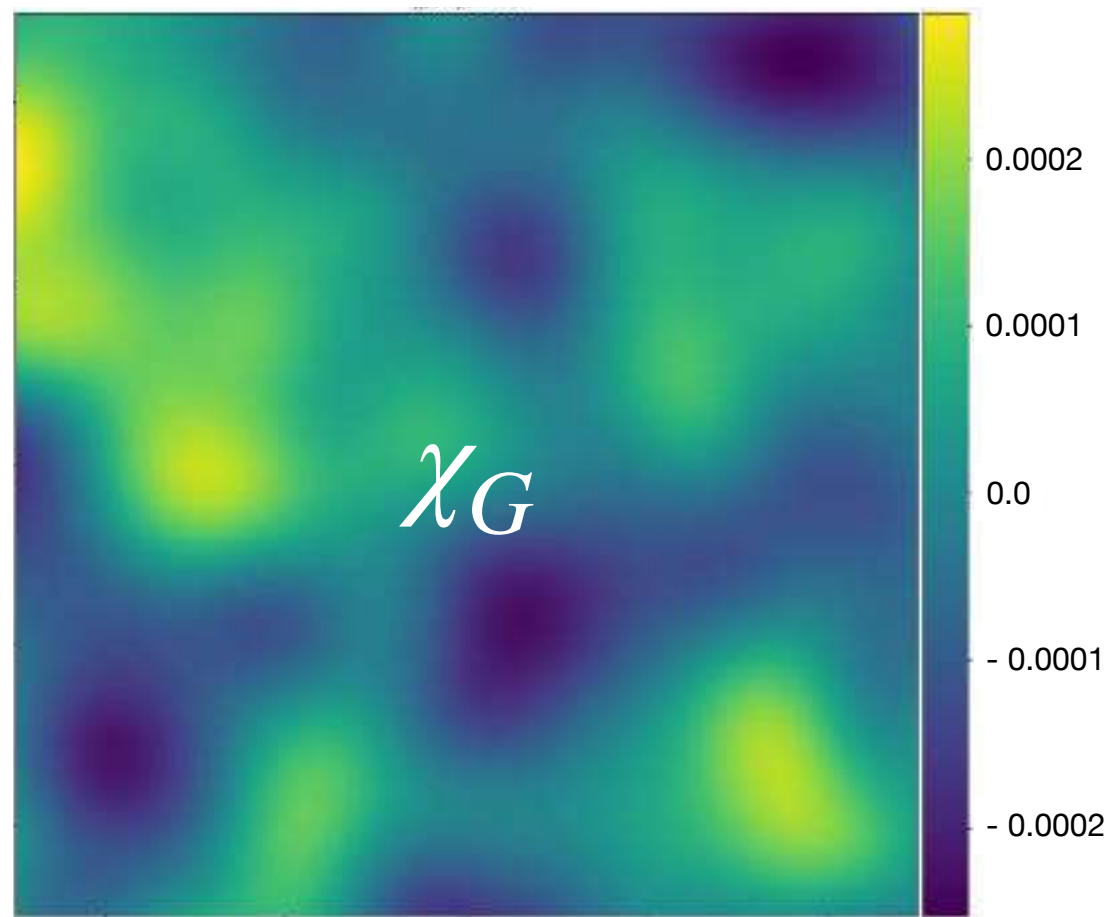
$$\zeta(\mathbf{x}) = \zeta_G(\mathbf{x}) + F_{\text{NL}} [\chi_G(\mathbf{x})]$$

I'm a functional,  
not a constant





# Other mechanisms generate non-Gaussianity from uncorrelated primordial fields coupling to observables via functional forms that don't fit the $f_{\text{NL}}$ series expansion approach



The transverse inflationary Gaussian field  $\chi_G$  where  $\Delta\zeta = F_{\text{NL}}[\chi_G]$

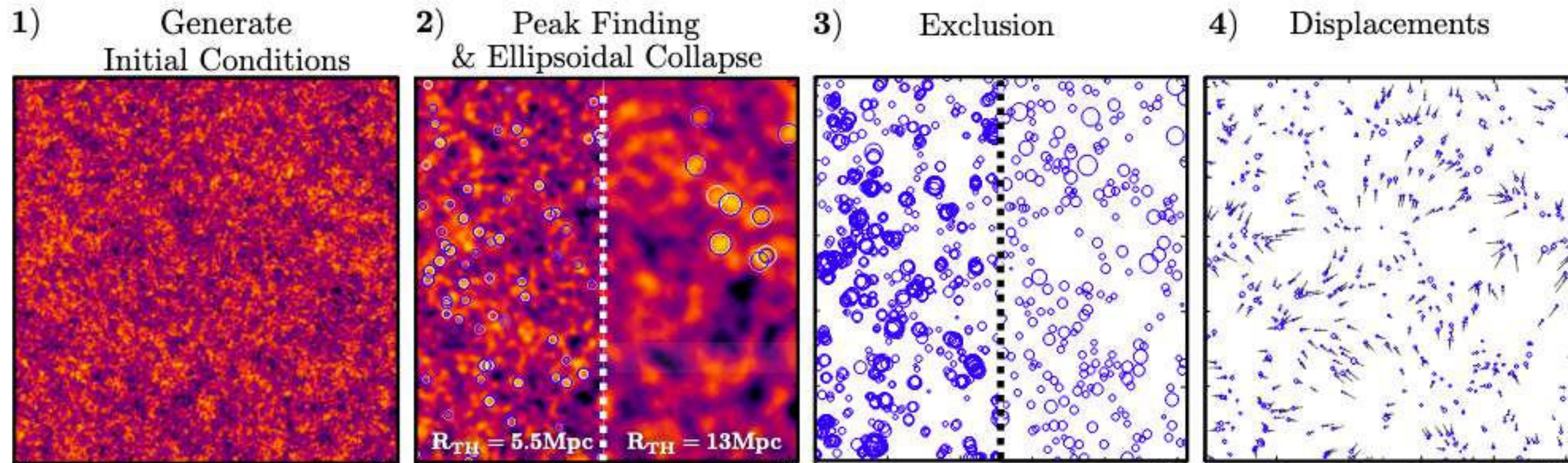


# The *Peak-Patch/WebSky2.0* pipeline

(And how can we isolate primordial non-Gaussianity from foregrounds?)



Dark matter halo catalogues are generated with the *Peak Patch* algorithm which uses RG flow and approximate dynamics to identify where structures will form based on an initial energy density.



Stein *et al.*, 2020  
(arXiv:1810.07727)

Start with a power spectrum describing matter distribution, generate realization of a random field with that power.

Identify where structures will form using peak finding and gravitational collapse of homogeneous ellipsoids at a series of real-space spherical top-hat filter scales.

Run a merging and exclusion algorithm to avoid double counting mass in overlapping patches.

Displace halos based on laplacian of initial fields, using low order perturbation theory.

The result is a catalogue of all DM halos above a threshold size.

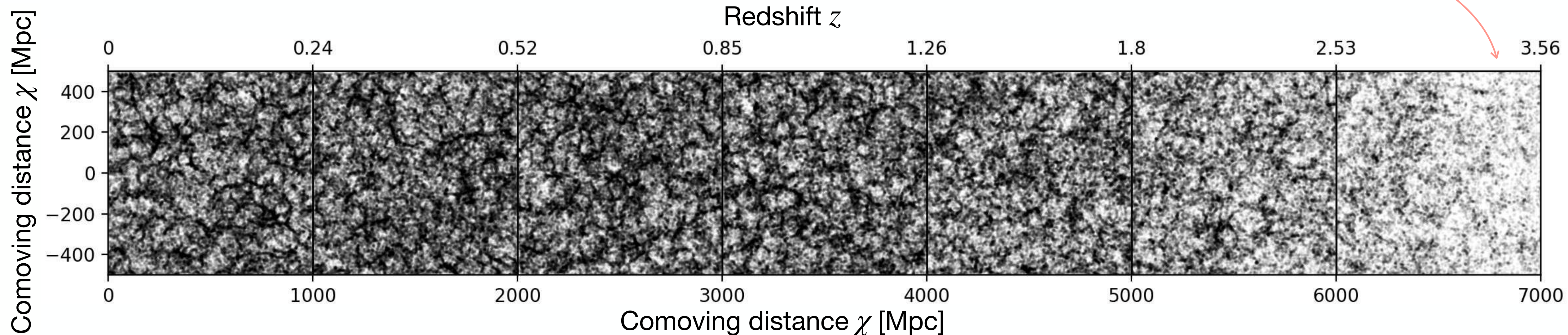
A major advantage is that *Peak Patch* DM halo catalogues can be run as light cones, meaning that halos at greater comoving distance will appear older, just as they do in observations. This as well as high computational efficiency and the ability to insert exotic initial conditions via power spectra are the main advantages of the *Peak Patch* approach.



***Peak Patch*** efficiently generates cosmological dark matter distributions and has native support for a diversity of non-Gaussian initial conditions.

**Gaussian DM halo catalogue**

Intermittent peaks at this characteristic scale especially visible at high redshift where halos are fewer and smaller



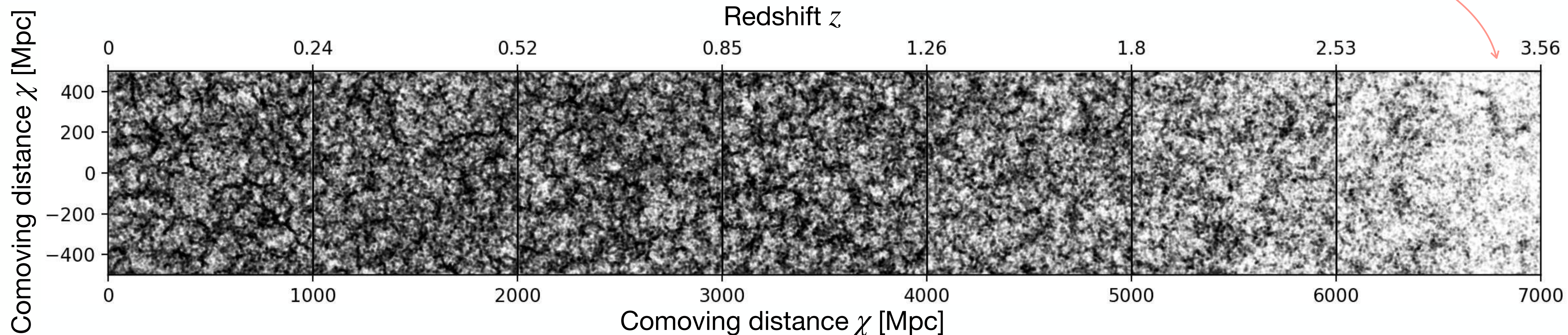
Peak Patch dark matter halo catalogues showing a 50 Mpc thick slab projected onto a plane (Carlson+23 in prep).



***Peak Patch*** efficiently generates cosmological dark matter distributions and has native support for a diversity of non-Gaussian initial conditions.

## Non-Gaussian DM halo catalogue

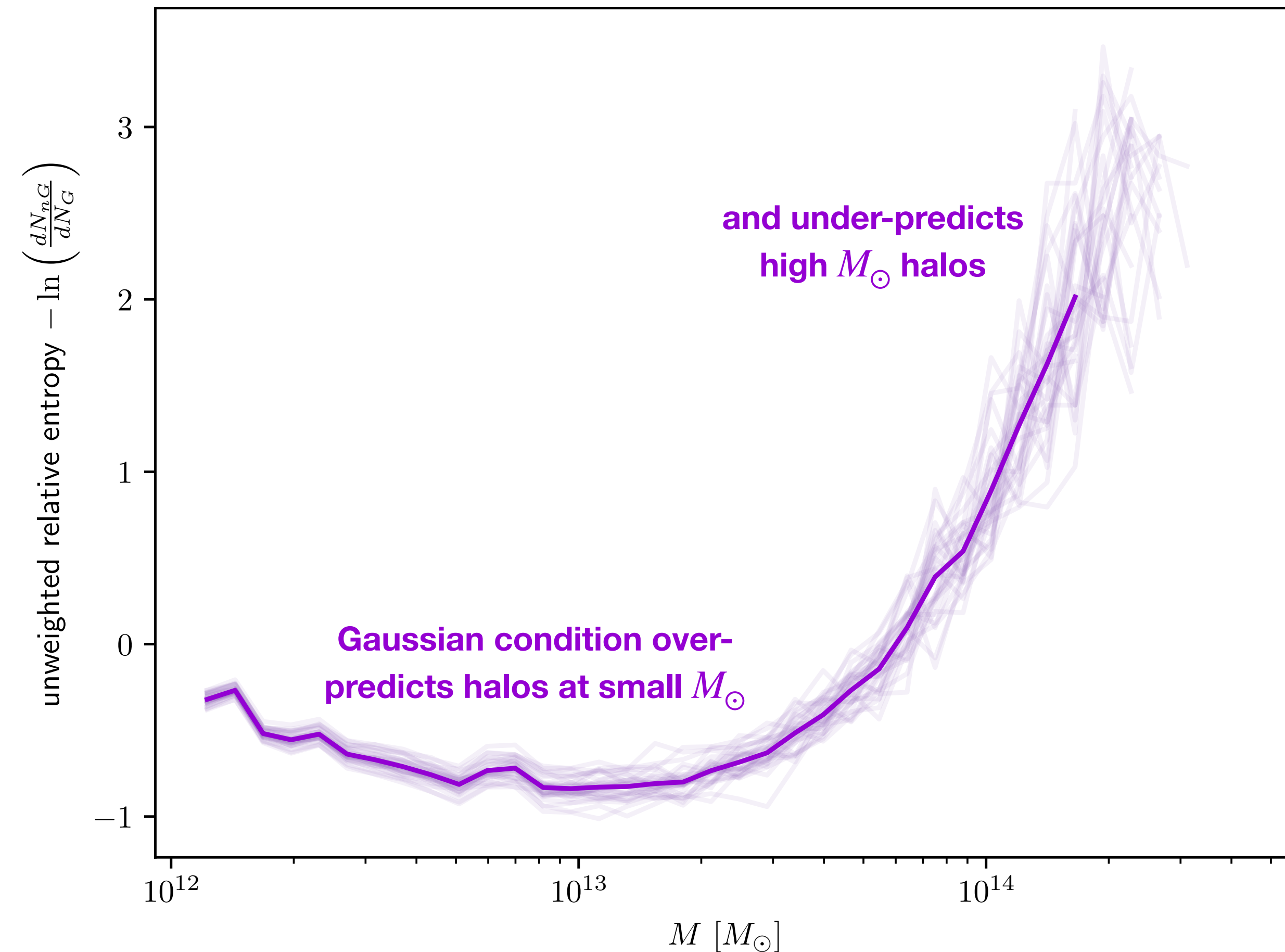
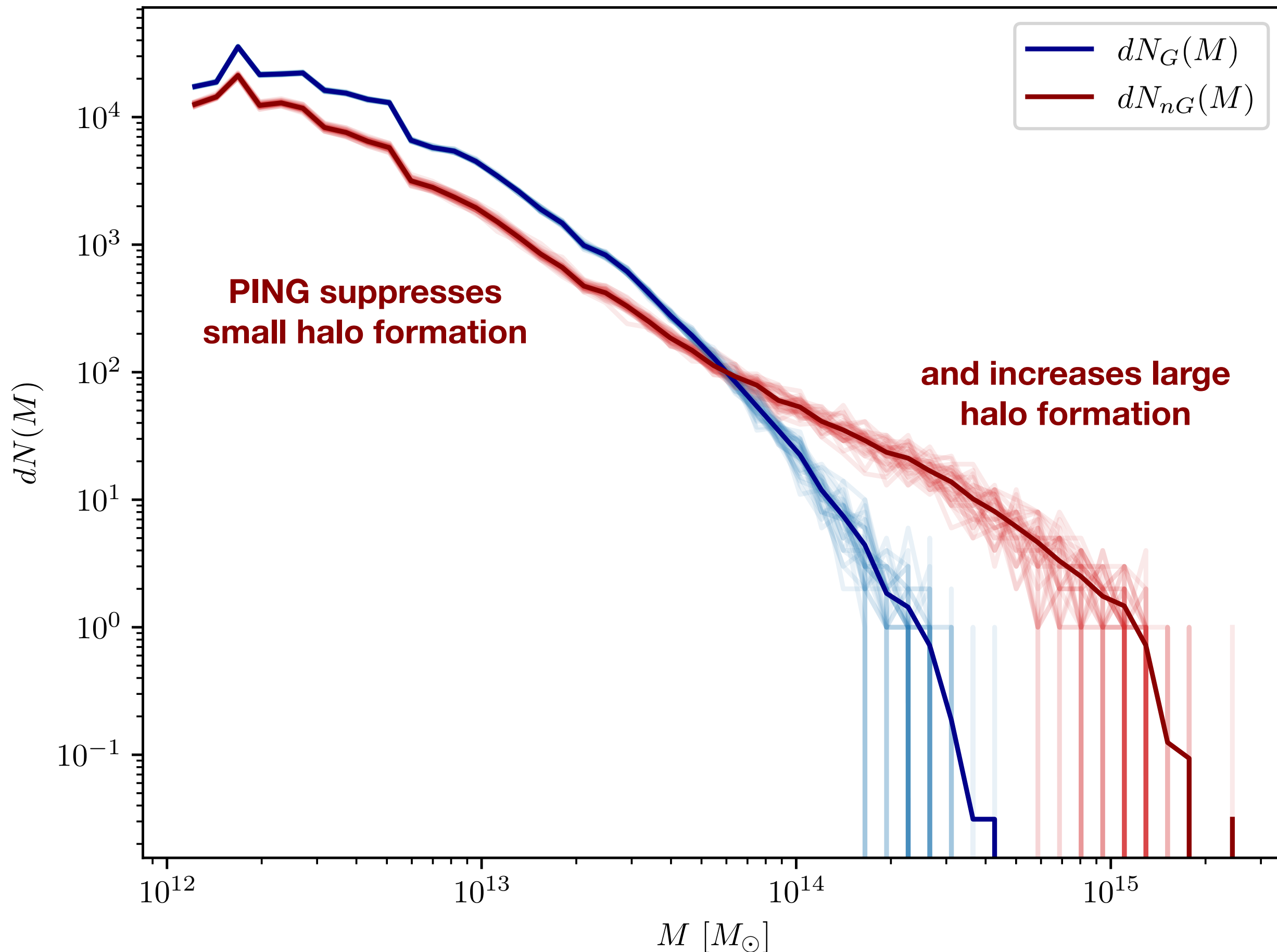
Intermittent peaks at this characteristic scale especially visible at high redshift where halos are fewer and smaller



Peak Patch dark matter halo catalogues showing a 50 Mpc thick slab projected onto a plane (Carlson+23 in prep).



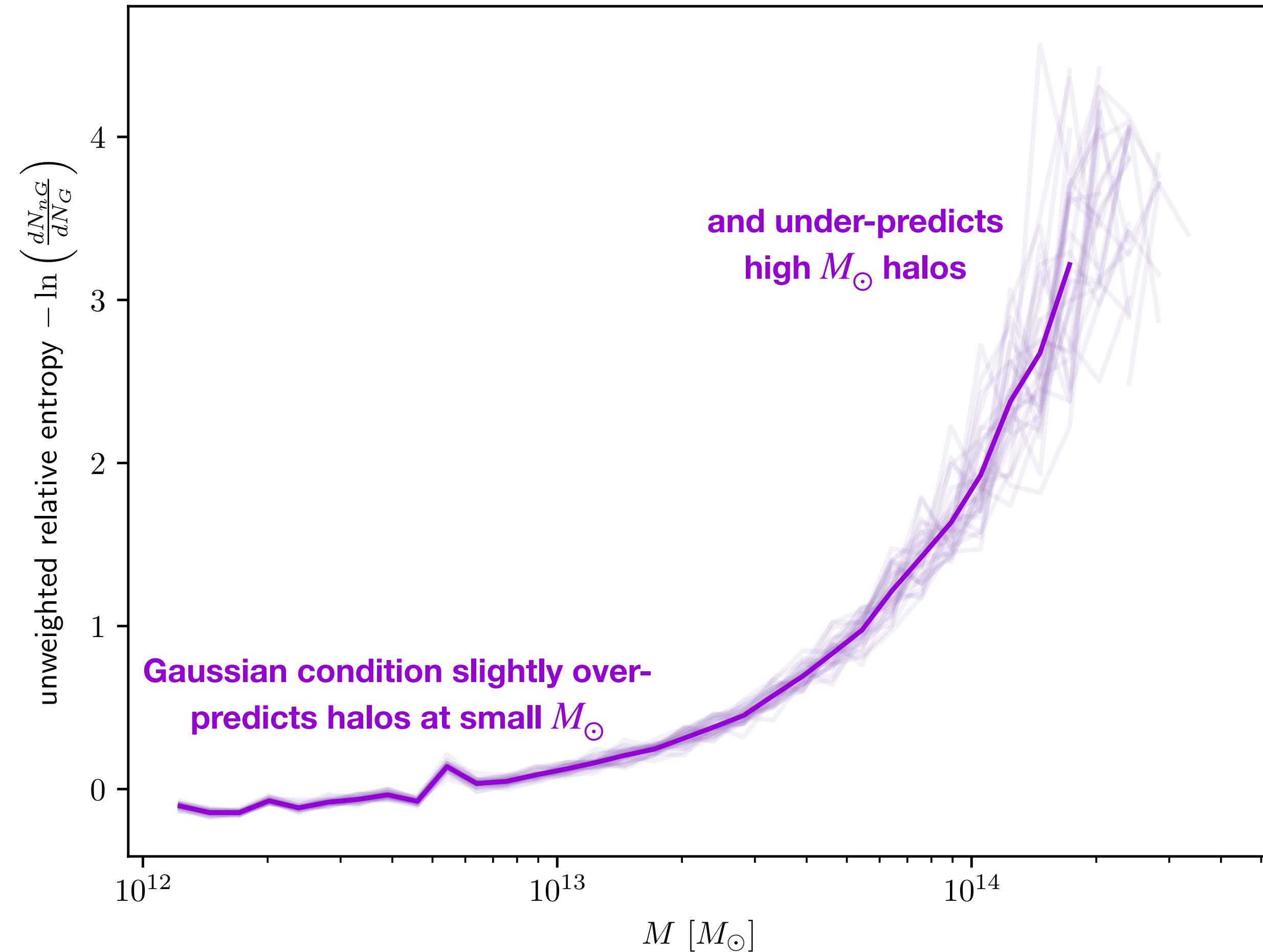
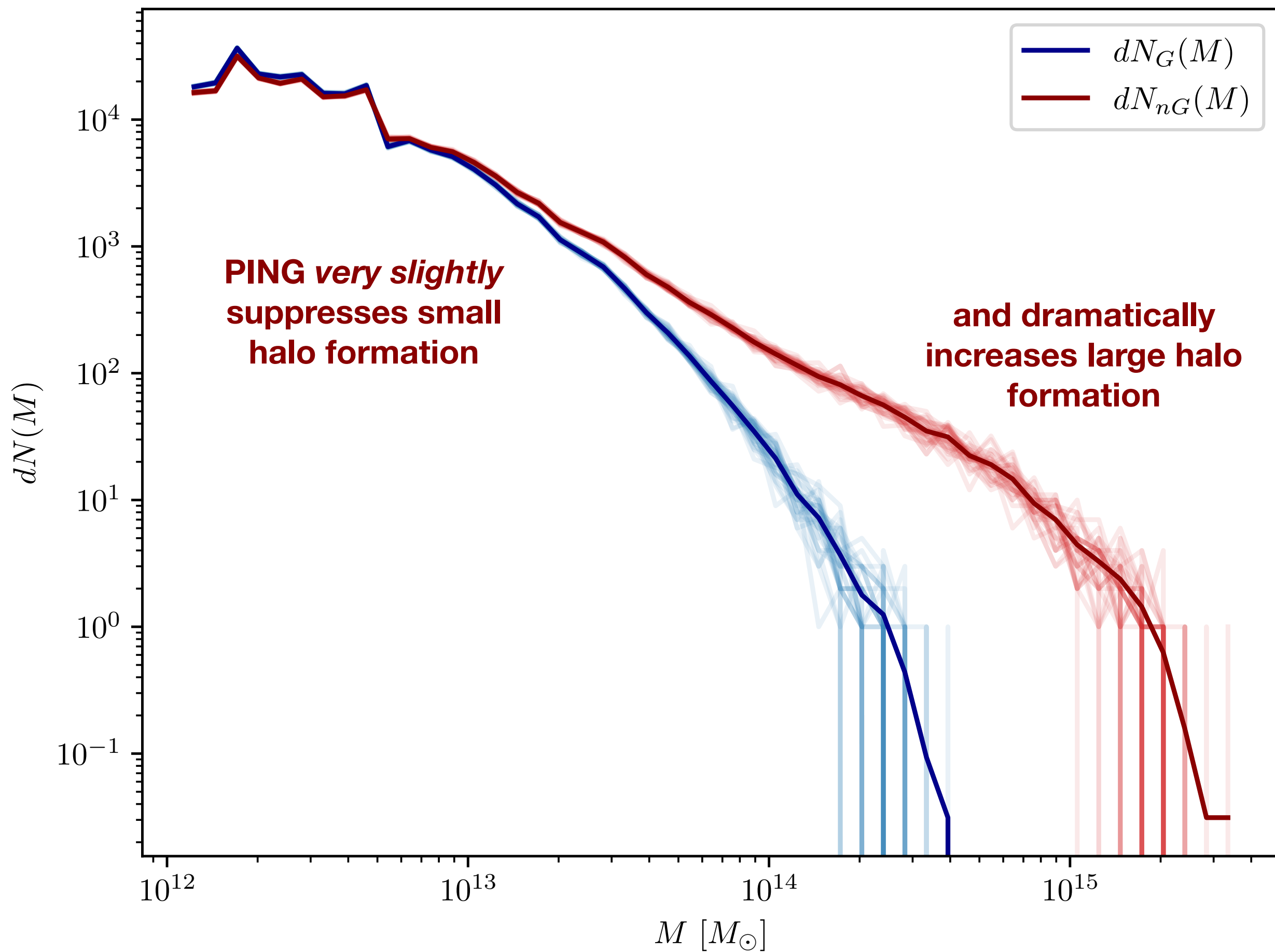
The halo mass function (HMF) is a summary statistic for DM halo distributions from *Peak Patch*. Averaging 32 statistically identical halo catalogues gives a clearer picture of the PING effect.



When we **normalize the Gaussian part** of the field  $\sigma_{8,G} = \sigma_8^{Planck18}$  we see suppression of low-mass halos and amplification of high-mass halos.



The halo mass function (HMF) is a summary statistic for DM halo distributions from *Peak Patch*. Averaging 32 statistically identical halo catalogues gives a clearer picture of the PING effect.

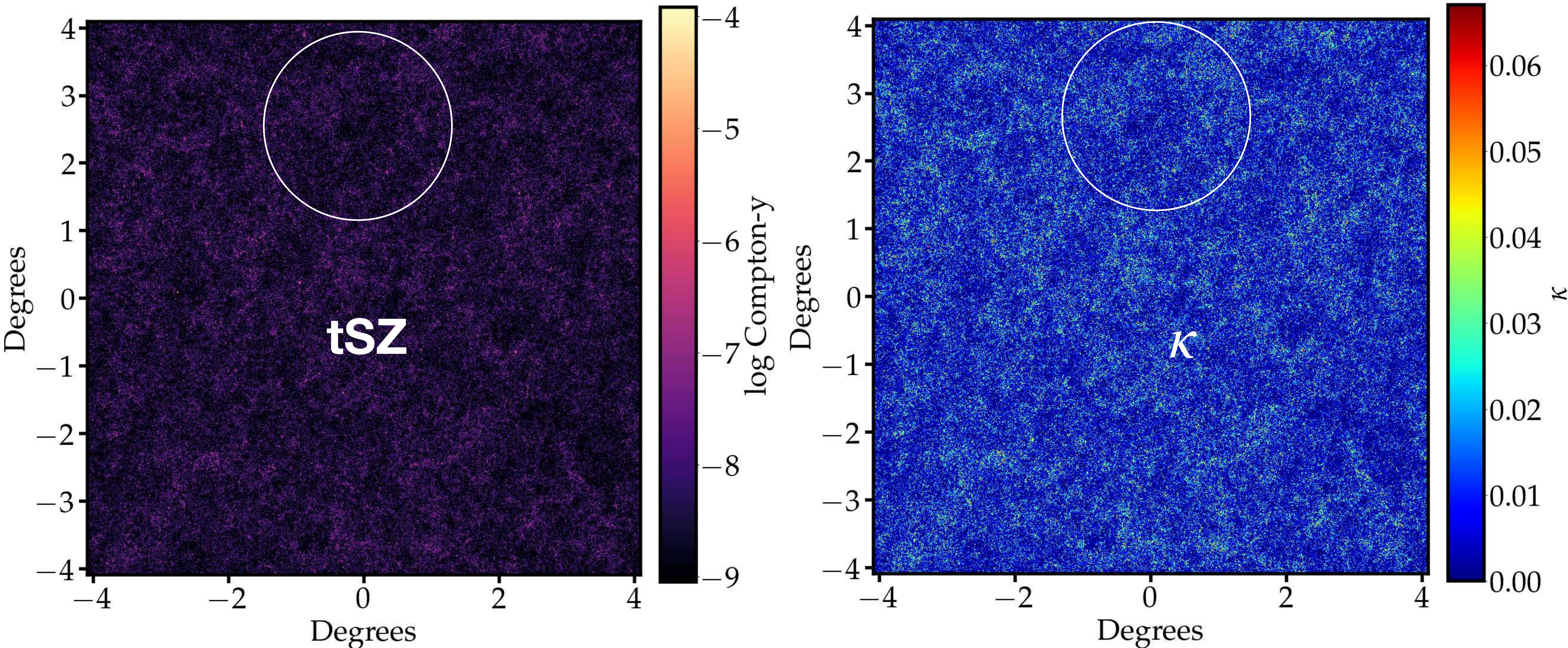


When we **normalize the total field**  $\sigma_8 = \sigma_8^{Planck18}$  we see suppression of low-mass halos and amplification of high-mass halos.



# WebSky models response functions to various observables, giving us the galaxy-halo connection. For **Gaussian** initial conditions:

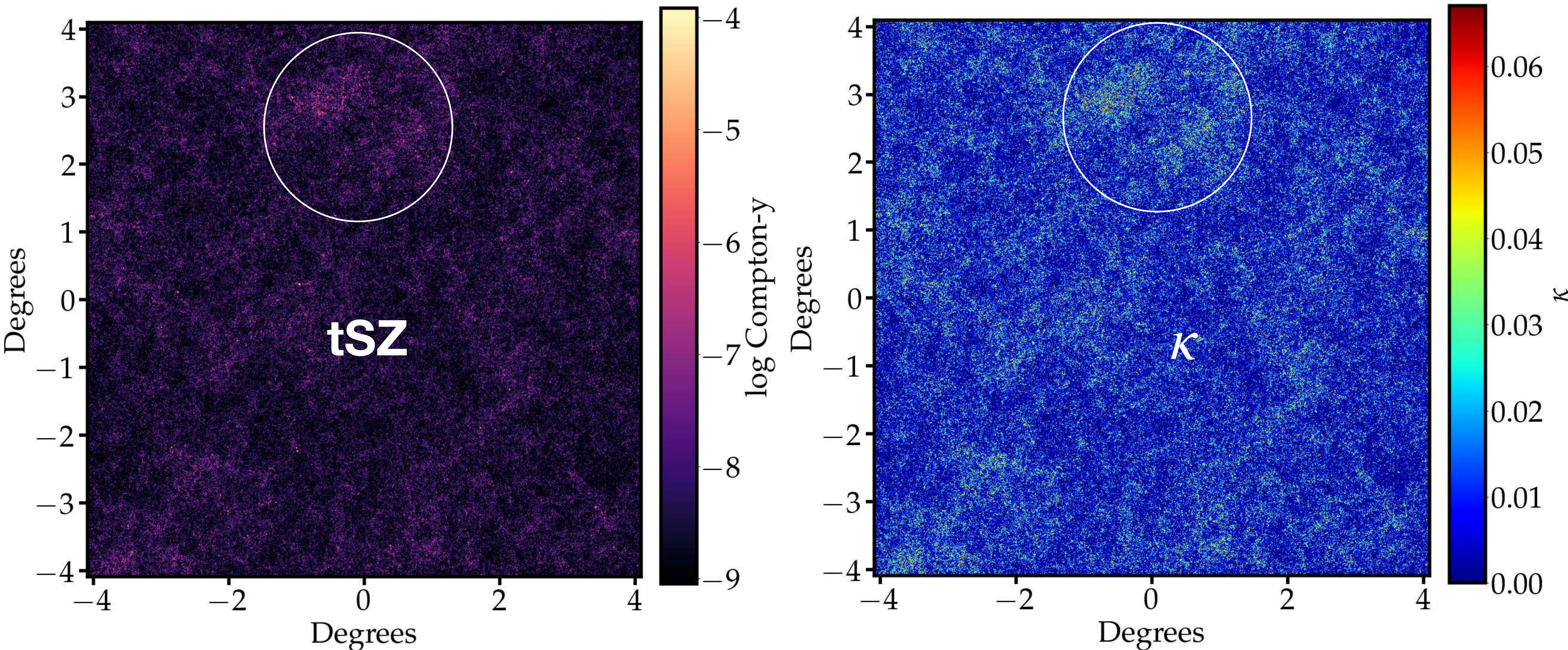
tSZ and kappa slices from  $z \sim 2.5$  to  $z \sim 3.5$





**WebSky models response functions to various observables, giving us the galaxy-halo connection. For **non-Gaussian** initial conditions:**

tSZ and kappa slices from  $z \sim 2.5$  to  $z \sim 3.5$





# Non-Gaussianity on the sky with the WebSky simulations

## CIB signal without PING

$\nu = 100$  Ghz

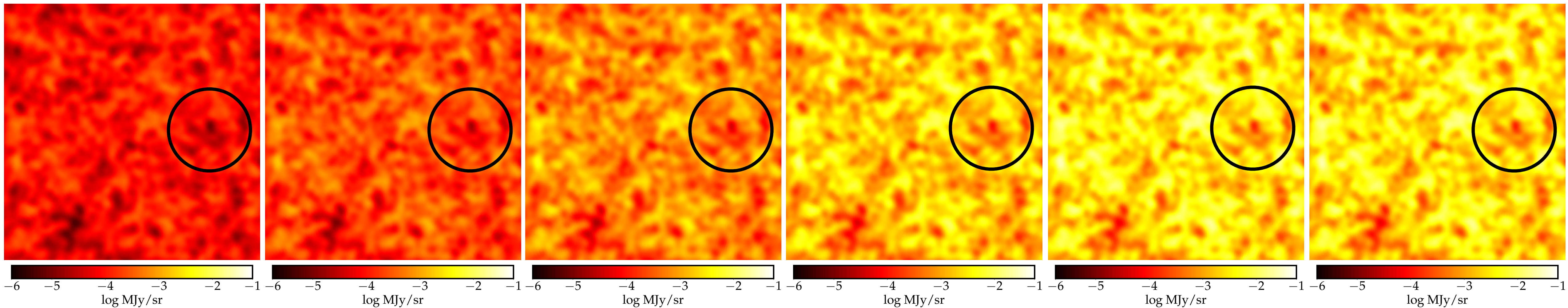
$\nu = 143$  Ghz

$\nu = 217$  Ghz

$\nu = 353$  Ghz

$\nu = 545$  Ghz

$\nu = 857$  Ghz



$8.182^\circ \times 8.182^\circ$  integrated CIB signal from  $z \in [2.53, 3.56]$  with Gaussian initial conditions.



# Non-Gaussianity on the sky with the WebSky simulations

## CIB signal with PING

$\nu = 100$  Ghz

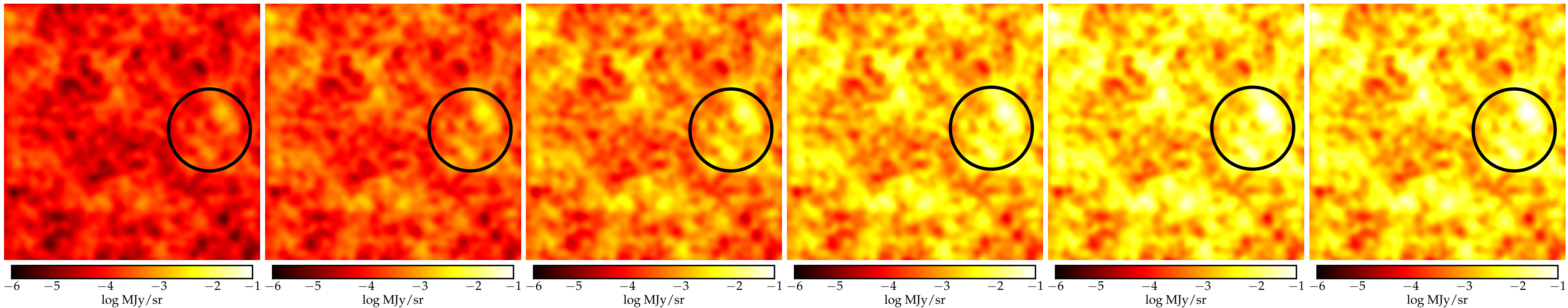
$\nu = 143$  Ghz

$\nu = 217$  Ghz

$\nu = 353$  Ghz

$\nu = 545$  Ghz

$\nu = 857$  Ghz



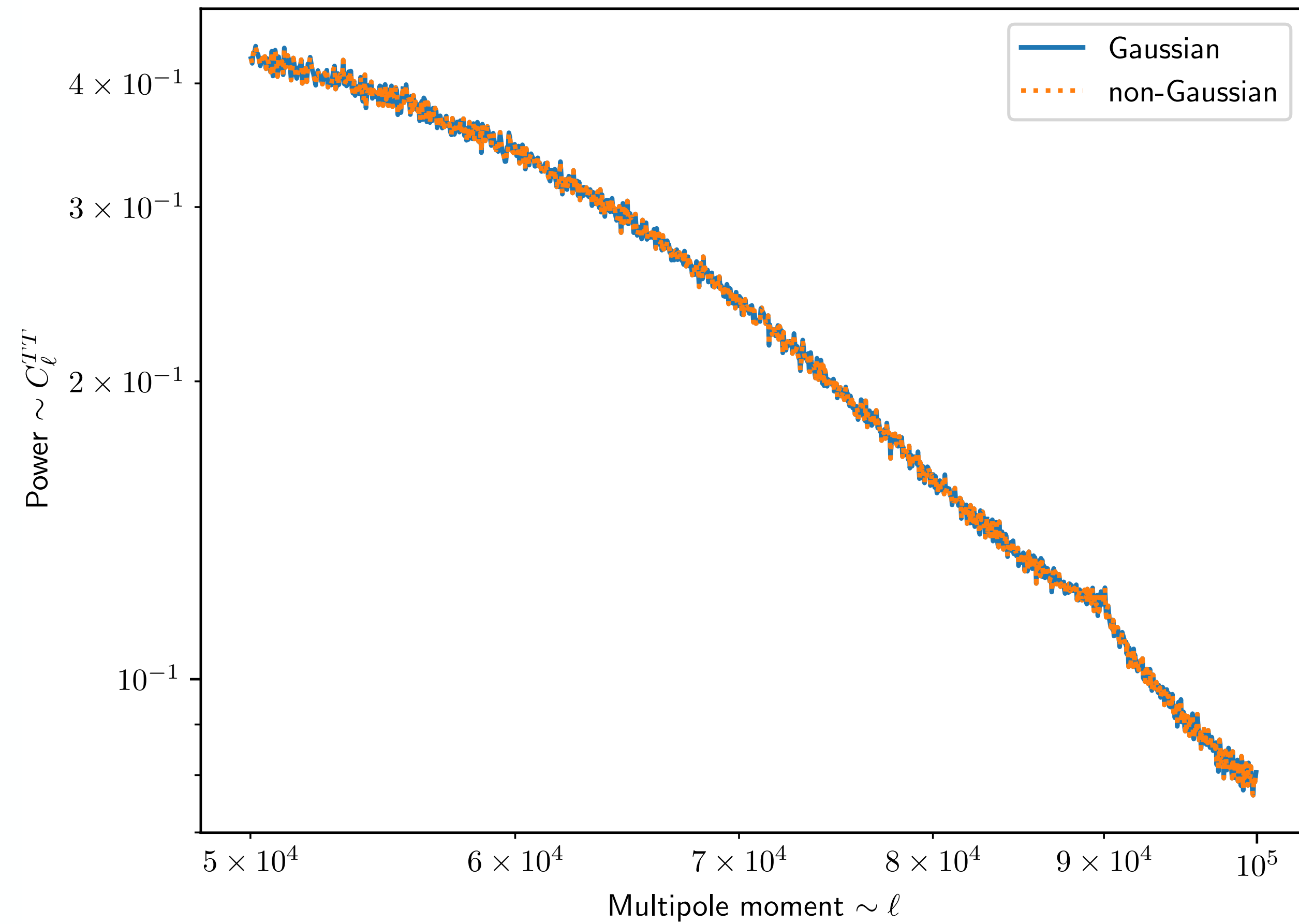
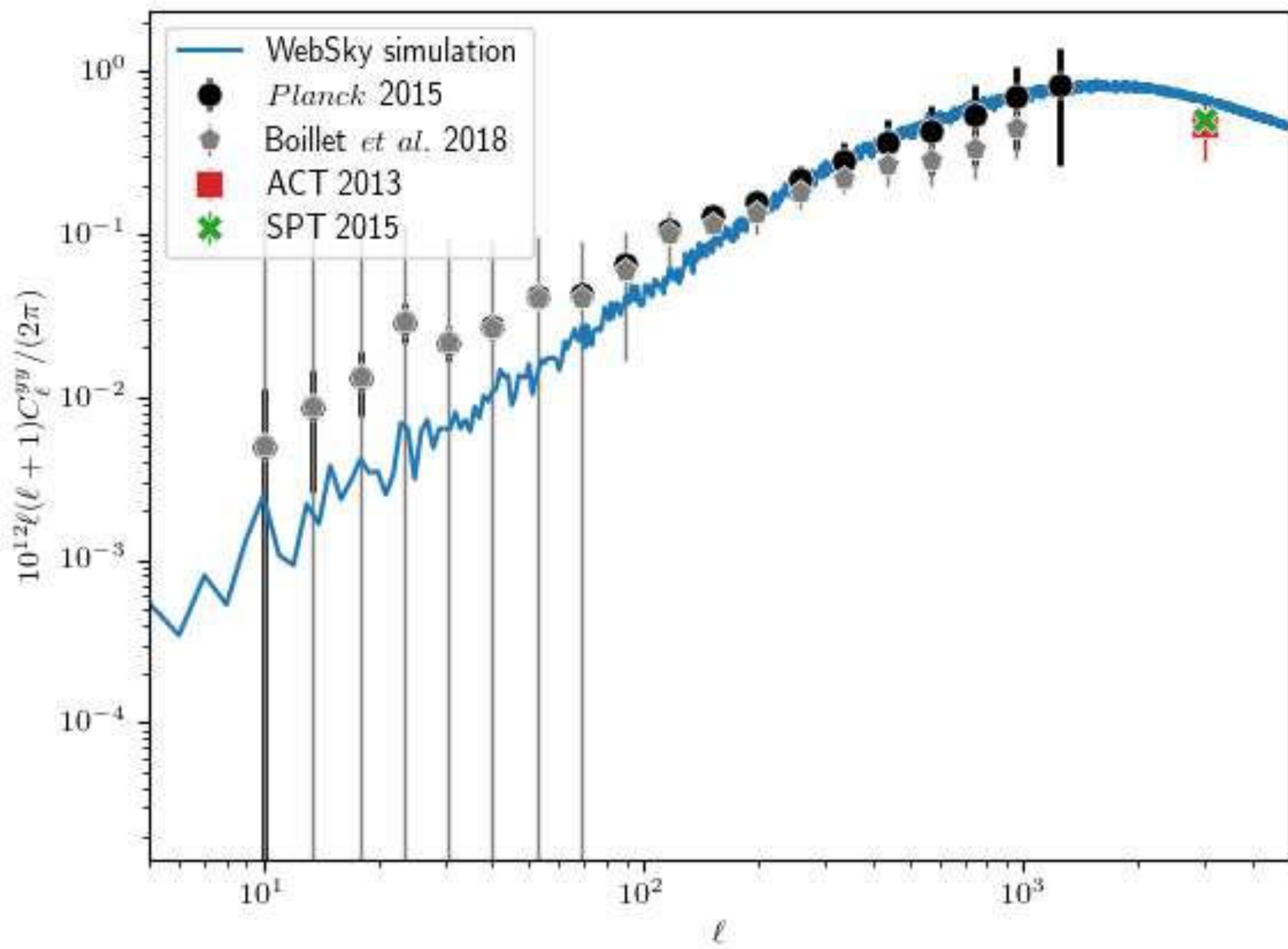
$8.182^\circ \times 8.182^\circ$  integrated CIB signal from  $z \in [2.53, 3.56]$  with non-Gaussian initial conditions.



# Constraining Inflation



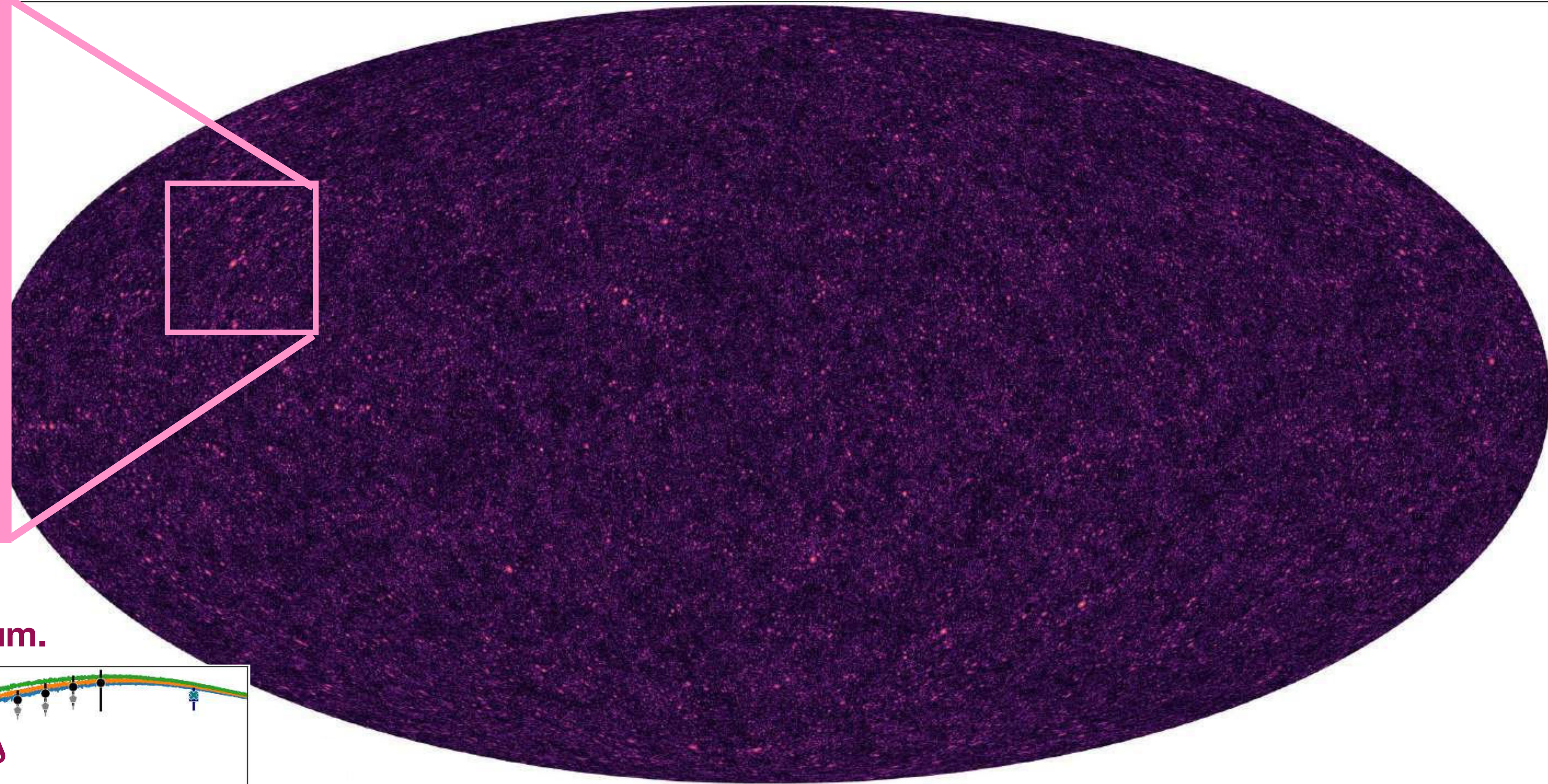
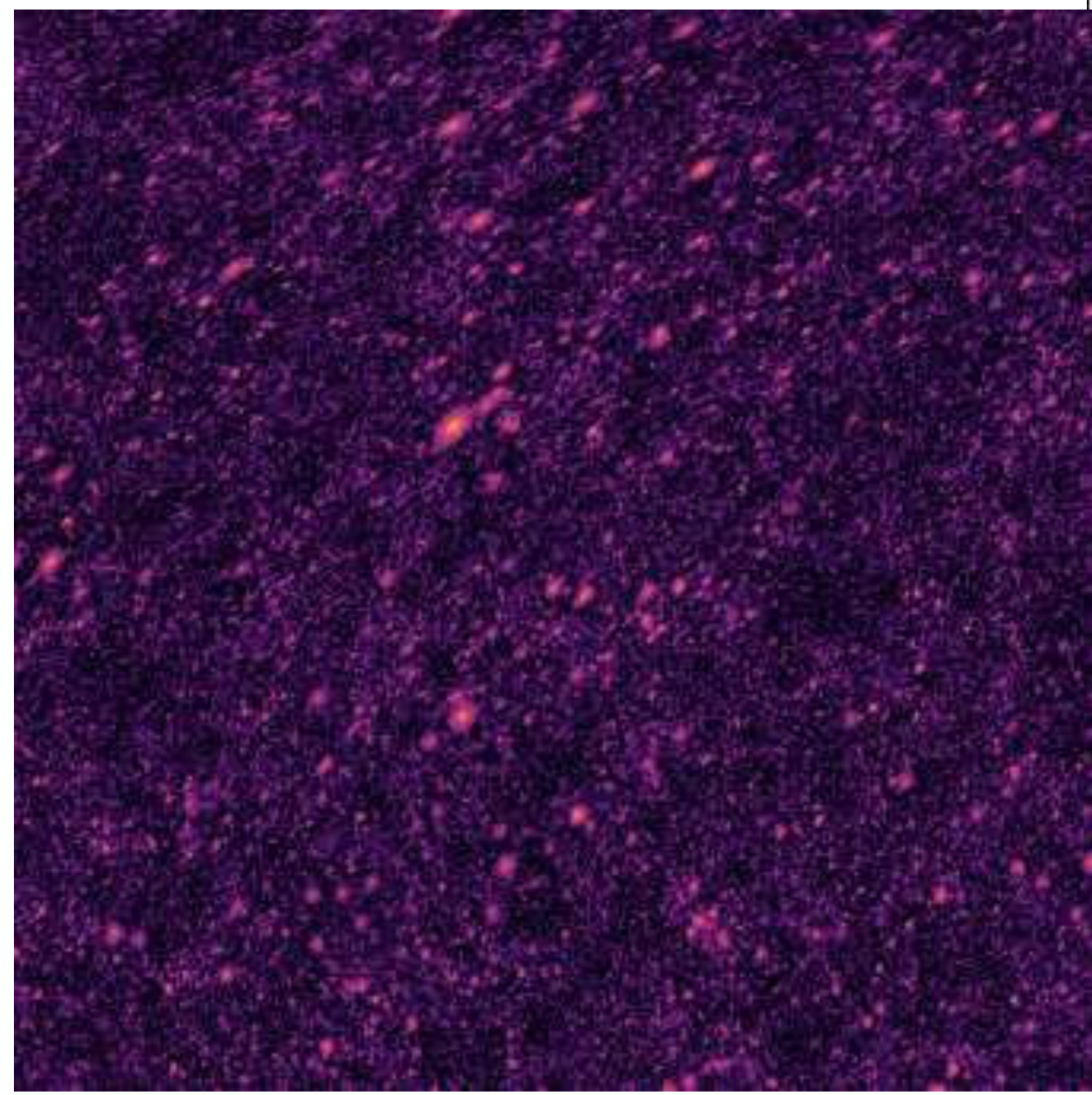
By measuring angular power spectra from these mock observables, we can directly compare the Gaussian and PING cosmologies to data.



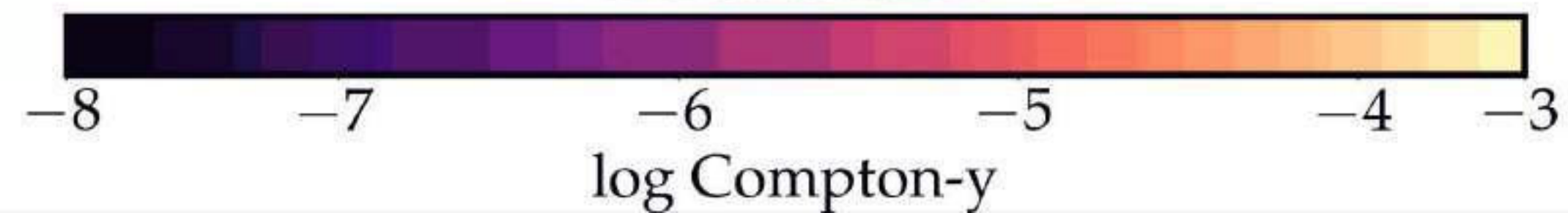
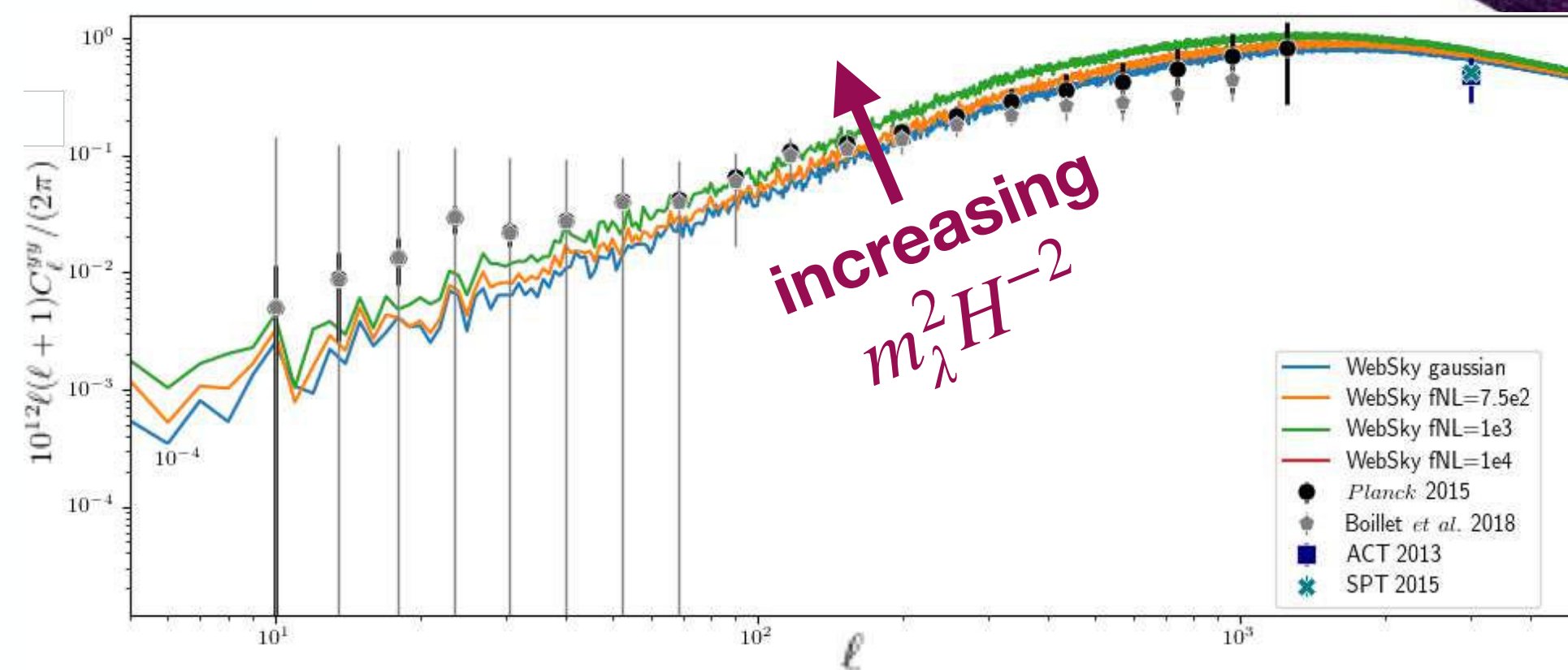
tSZ and CIB angular power spectra in strong agreement with the Gaussian case which was validated by Stein et al. [1810.07727]



Increasing the strength  $m_\lambda^2 H^{-2}$  of the PING instability gradually causes more clustering, which is visible on the sky.



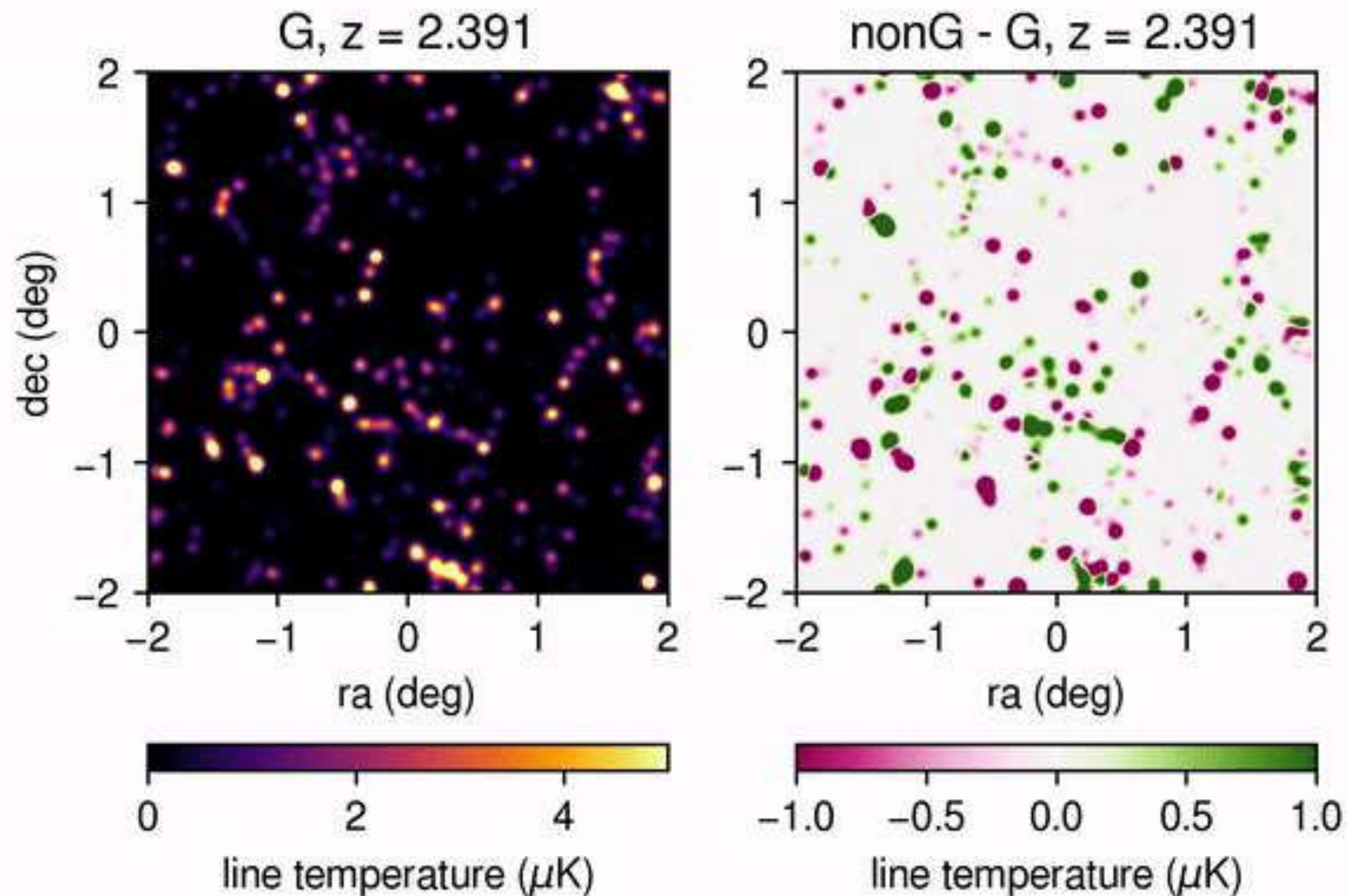
This causes a subtle change in the power spectrum.



Upcoming Public *WebSky* 2.0 mocks will feature a suite of non-Gaussian cosmologies, we (may) take requests



**Non-Gaussian effects in line-intensity maps are clearly visible when we subtract a run made from a halo catalogue with purely Gaussian initial conditions.**



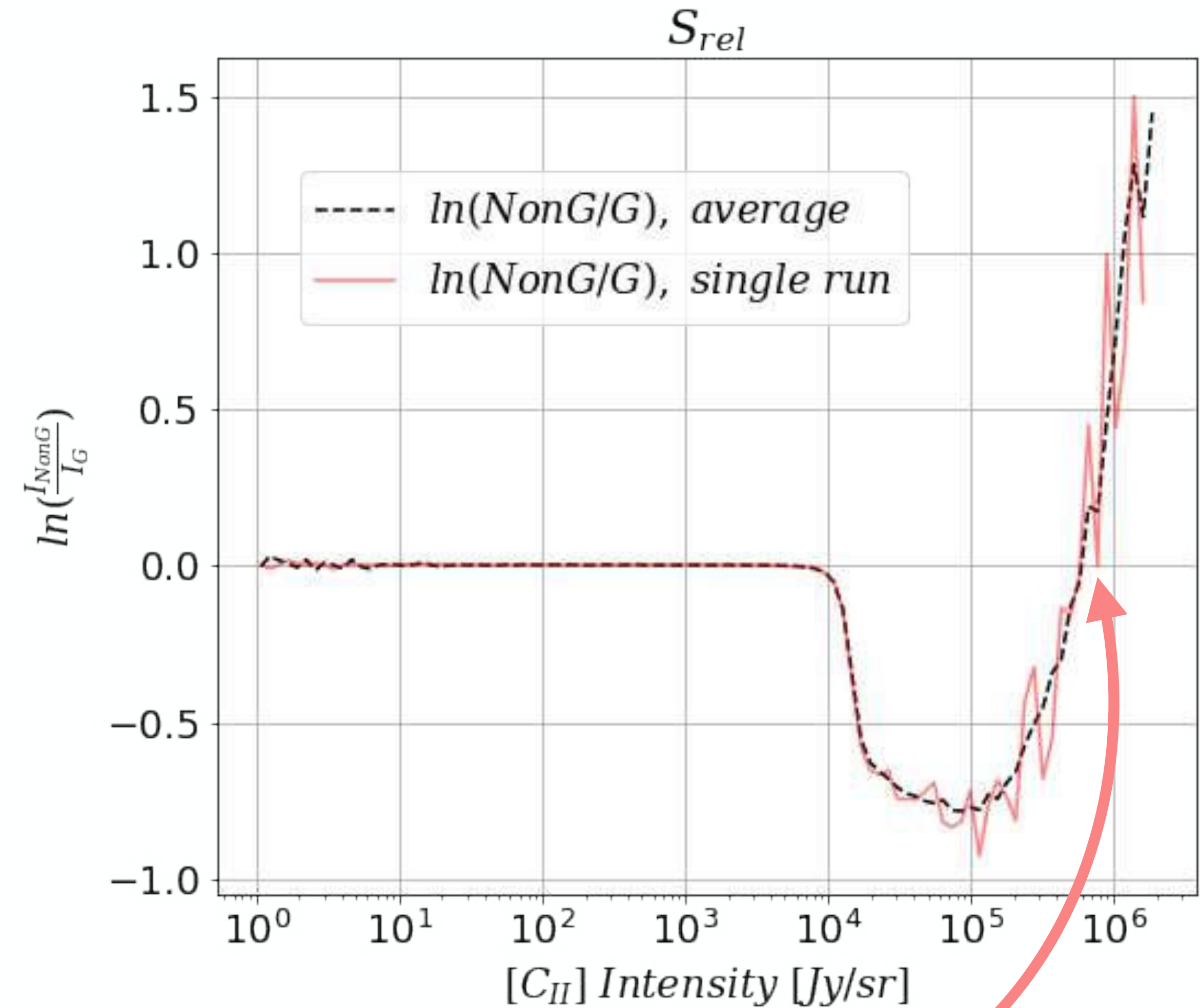
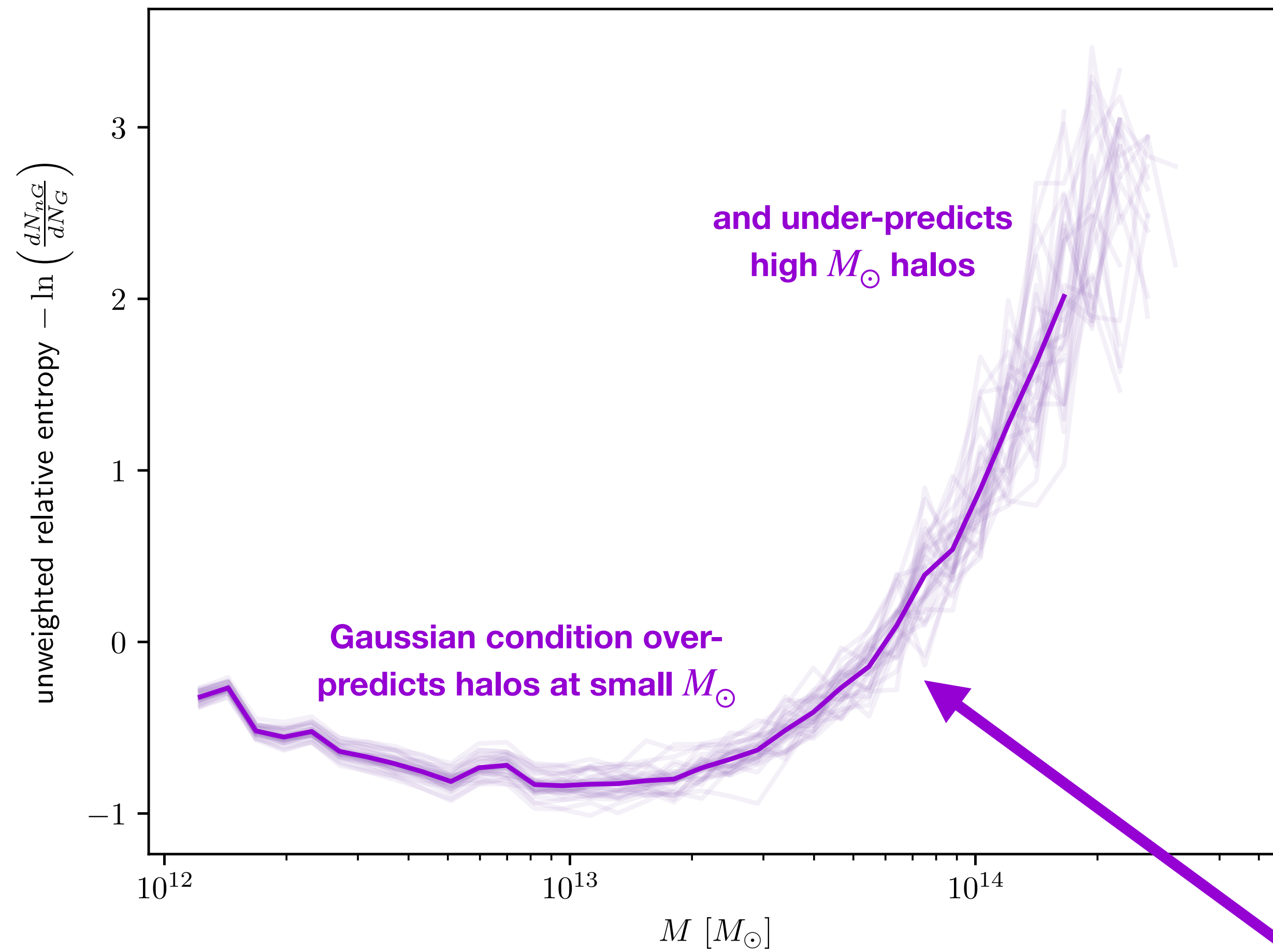
## Fly-through CO line intensity maps

with and without the inflaton traversing an instability during inflation (Chung *et al.* 2023, in prep).

Non-Gaussian effect clearly visible in  $C_{II}$  signal.



# The relative entropy of $C_{\text{II}}$ intensity matches that of halos



We see the same sign change in relative entropy in the **halos number densities** and in resultant  **$C_{\text{II}}$  intensity**.



**We are making updates to the *WebSky* mapmaking pipeline, working toward a public release of *WebSky2.0* mocks featuring unprecedented resolution full-sky maps needed for upcoming surveys for cosmologies with a suite of Gaussian and non-Gaussian initial conditions.**

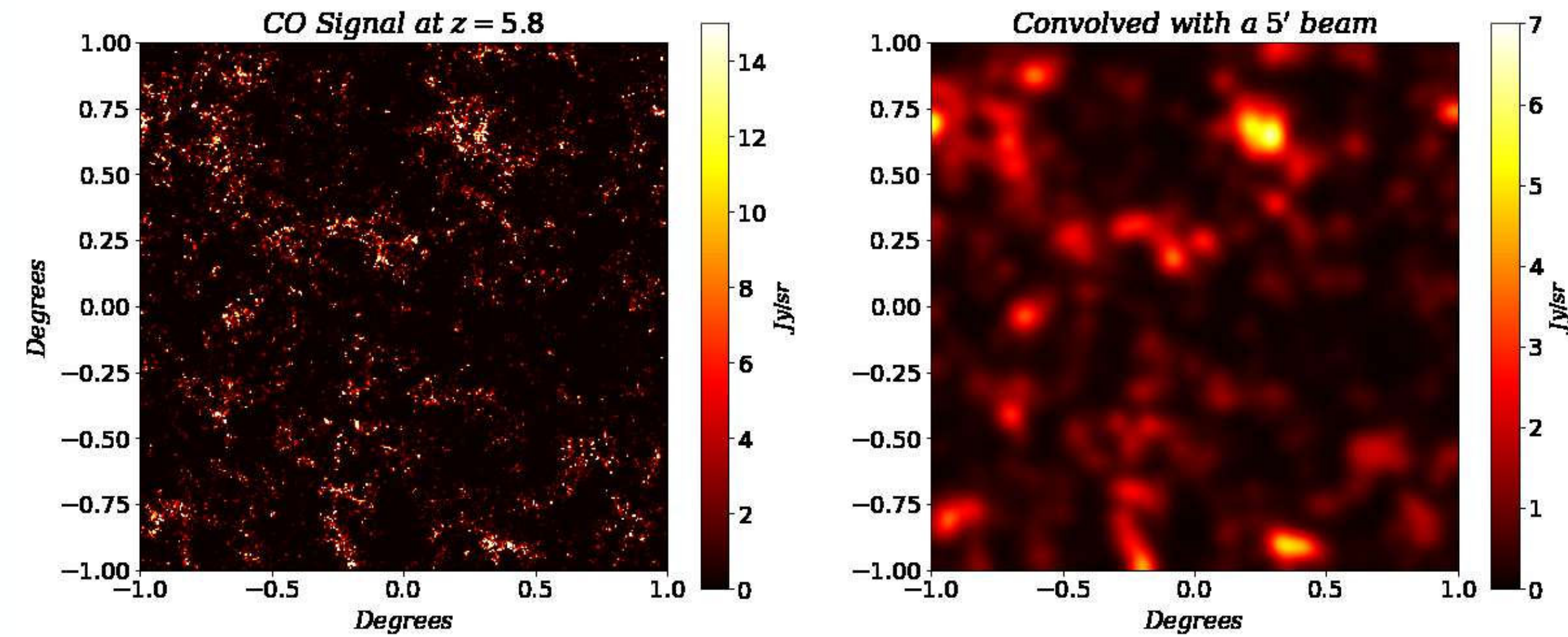
- Relativistic corrections to tSZ (Zack Li)
- Overhaul of CIB spectral energy distributions (Dongwoo Chung)
- Post-Born approximation to lensing (Nate Carlson)
- Optimizing for computer architecture to make the largest possible halo catalogues (Nate Carlson)

These mocks are necessary for next-gen surveys like SO and CCAT-prime, which have much greater angular resolution and will require halo masses below  $M_{200m} \sim 10^{12} M_{\odot}$ , the resolution which existing *WebSky* catalogues targeted.

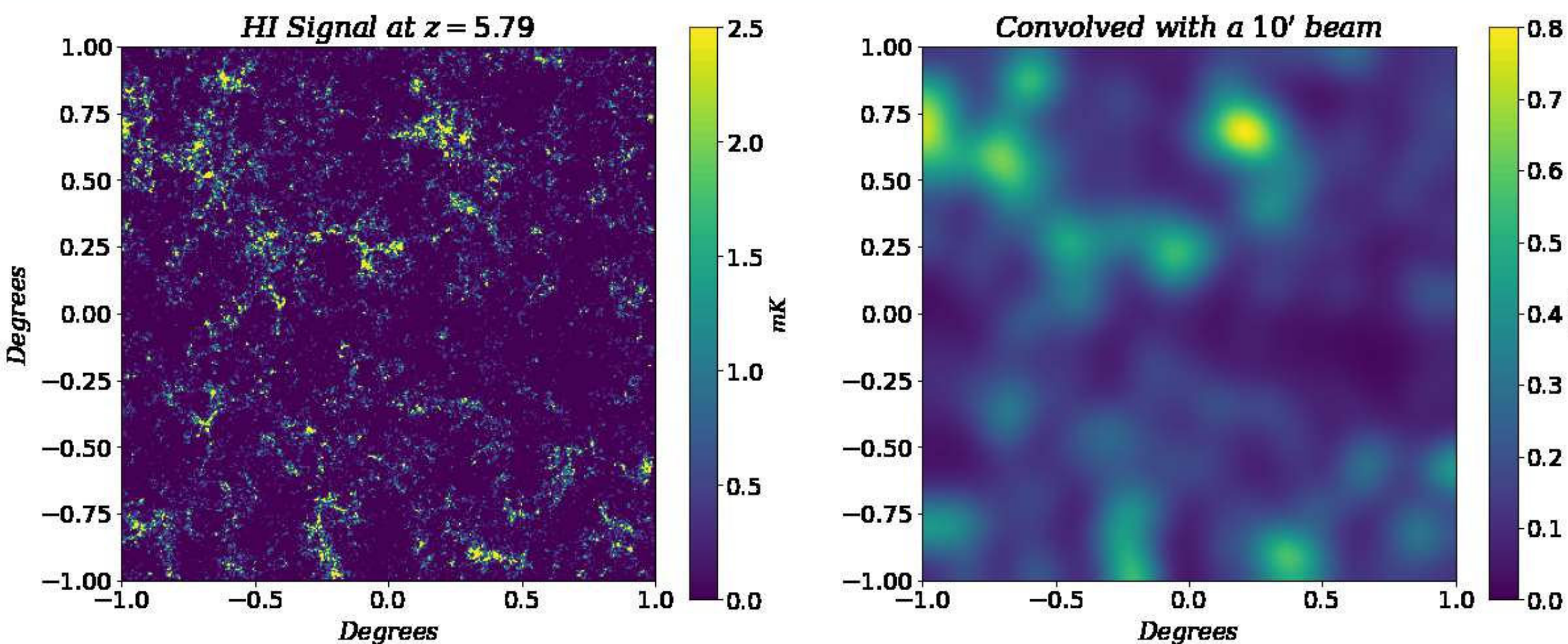


# Upcoming surveys need mocks at unprecedentedly high resolutions. We will deliver these.

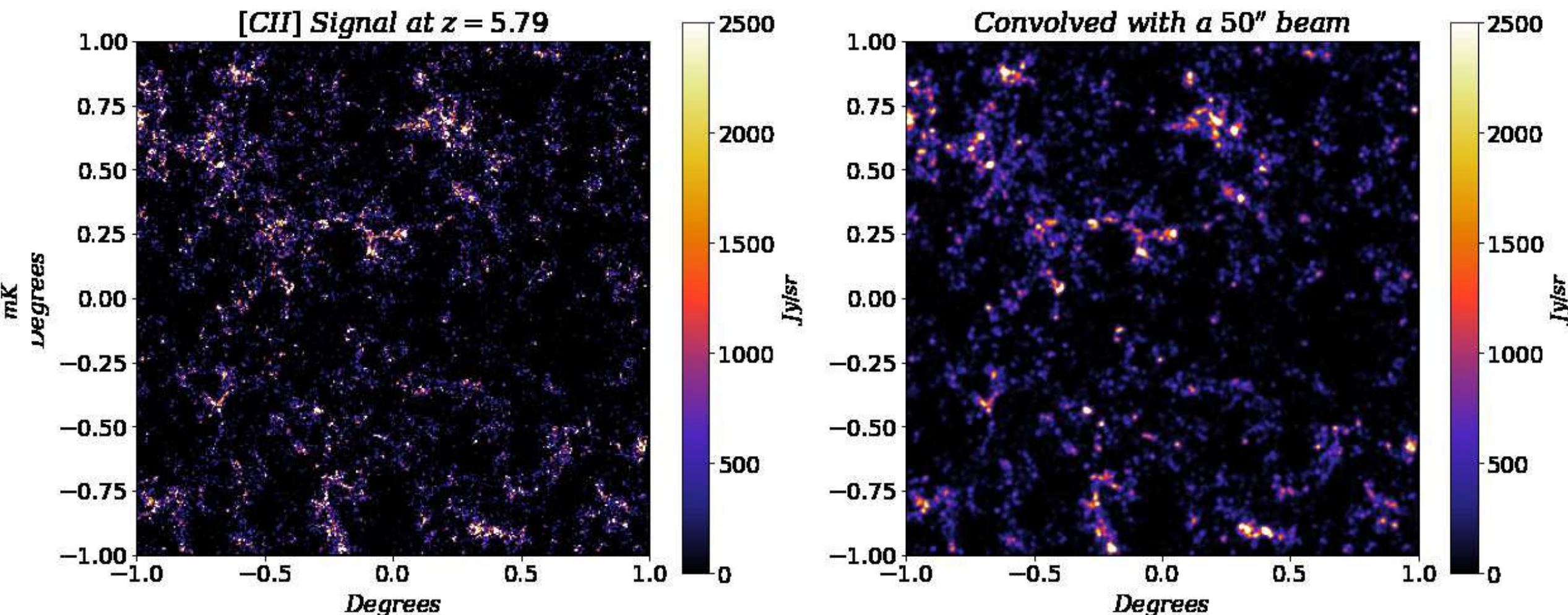
CO signal convolved with a COMAP beam.



HI 21cm signal convolved with a CHORD beam.



[CII] signal convolved with a CCAT-prime beam.

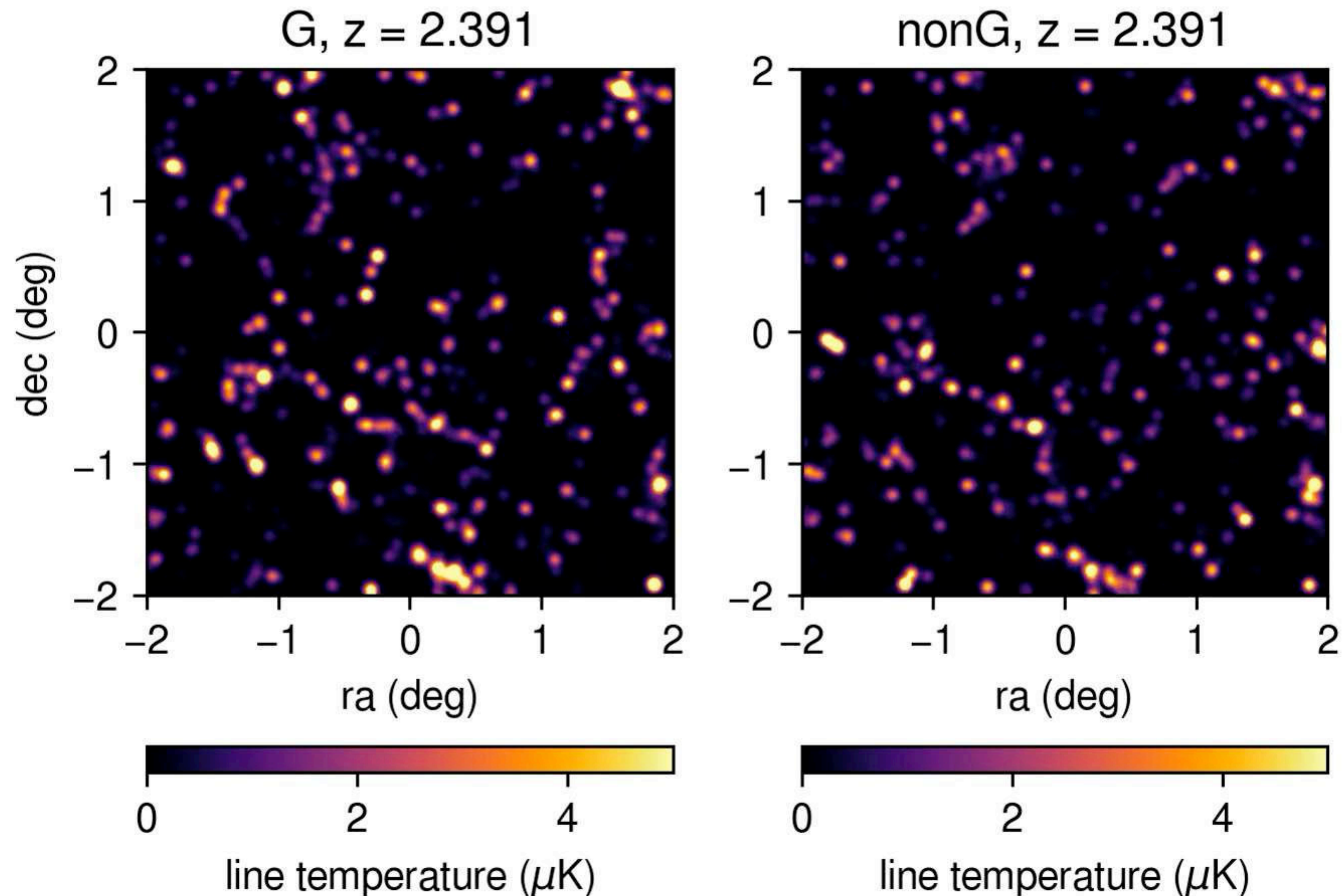


Fly-through videos courtesy of Chung *et al.* 2023 in prep.



# Conclusion

- The (mass) Peak-Patch/WebSky pipeline is well-suited for mocking universes with any non-Gaussian initial conditions.
- WebSky mocks can be used to put constraints on multi-field inflation models.
- We will be updating the existing public WebSky catalogues to include various non-Gaussian models. If you have a favourite model, let us know, we may include it!



## Fly-through CO line intensity maps

with and without the inflaton traversing an instability during inflation  
(courtesy of Dongwoo Chung)

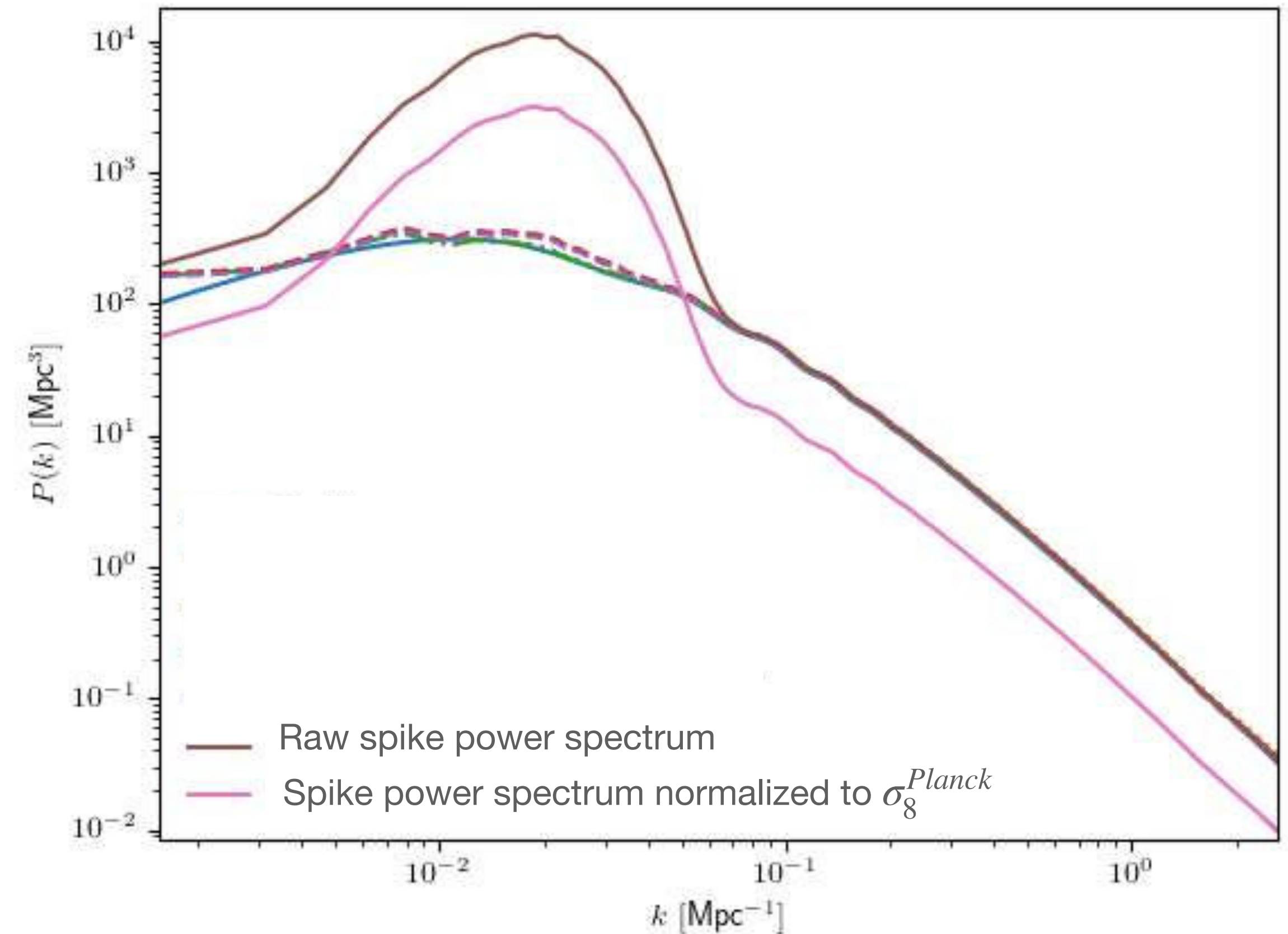




# Relative power is a better measure of the amplitude of non-Gaussianity than $f_{\text{NL}}$

$$\zeta(\mathbf{x}) = \frac{\sigma_8^{\text{Planck}}}{\sigma_8^{\text{ng}}} \left[ \zeta_G(\mathbf{x}) + F_{\text{NL}} [\chi_e(\mathbf{x})] \right]$$

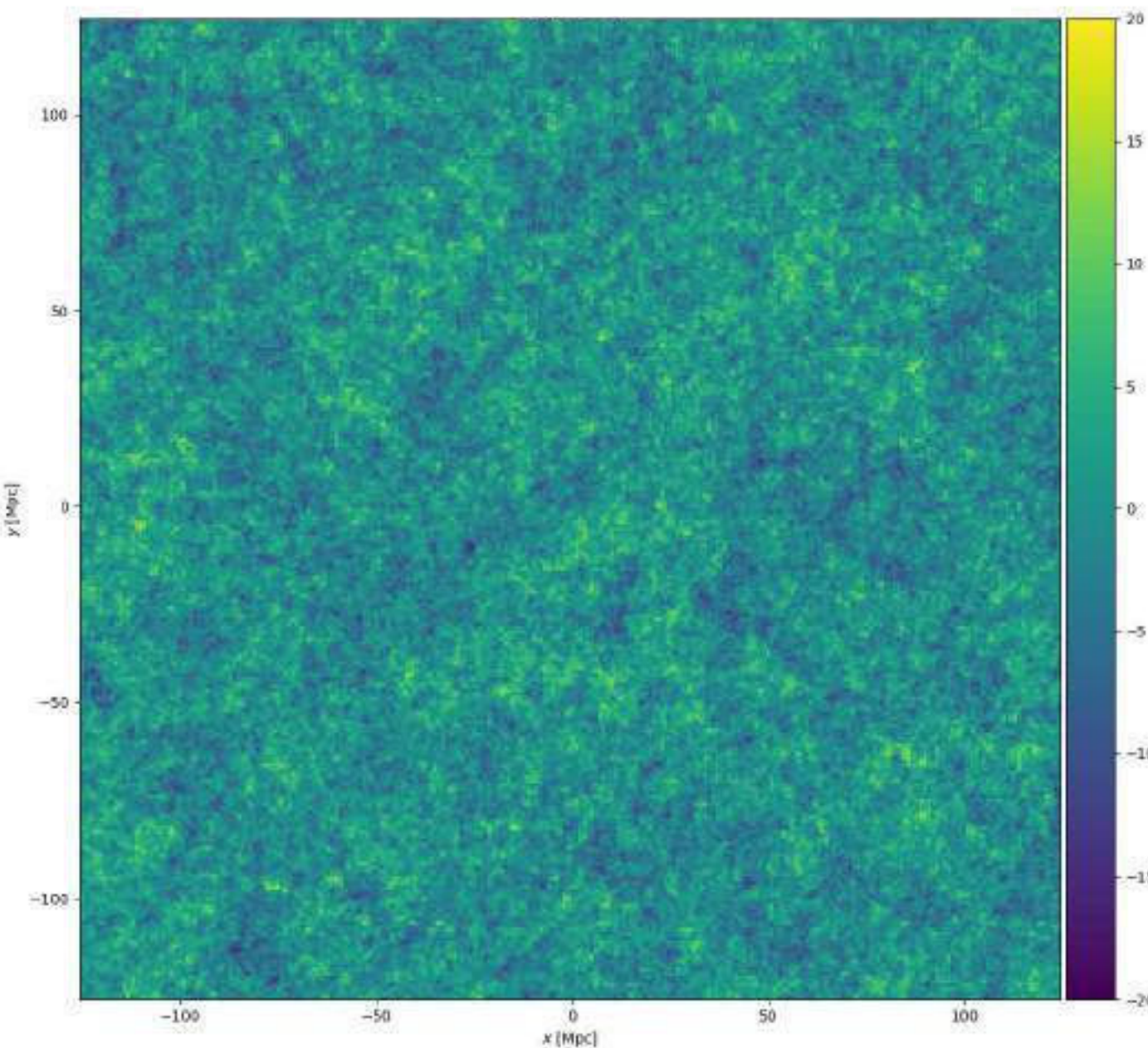
Where  $\sigma_{8,\text{obs}}$  is the standard deviation in the density perturbations  $\delta(\mathbf{x})$  smoothed at a scale of  $8 h^{-1} \text{Mpc}$  so we can use the *Planck* result for instance.





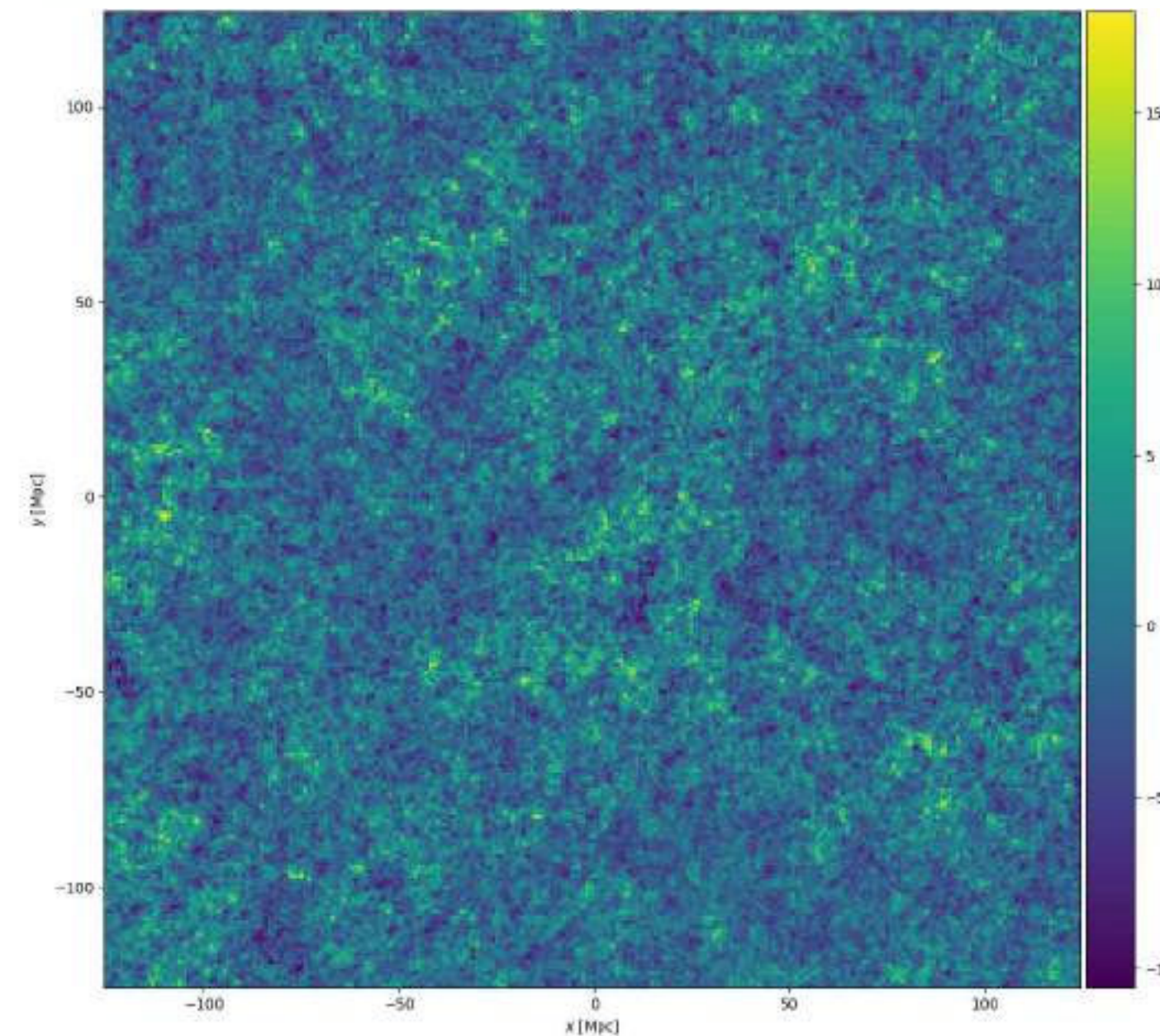
**There are other mechanisms that can generate non-Gaussianity that is not correlated to the underlying Gaussian field. In such cases, similar “ $f_{\text{NL}}$ ” give considerably less effect.**

Gaussian overdensity  $\delta_G(\mathbf{x})$



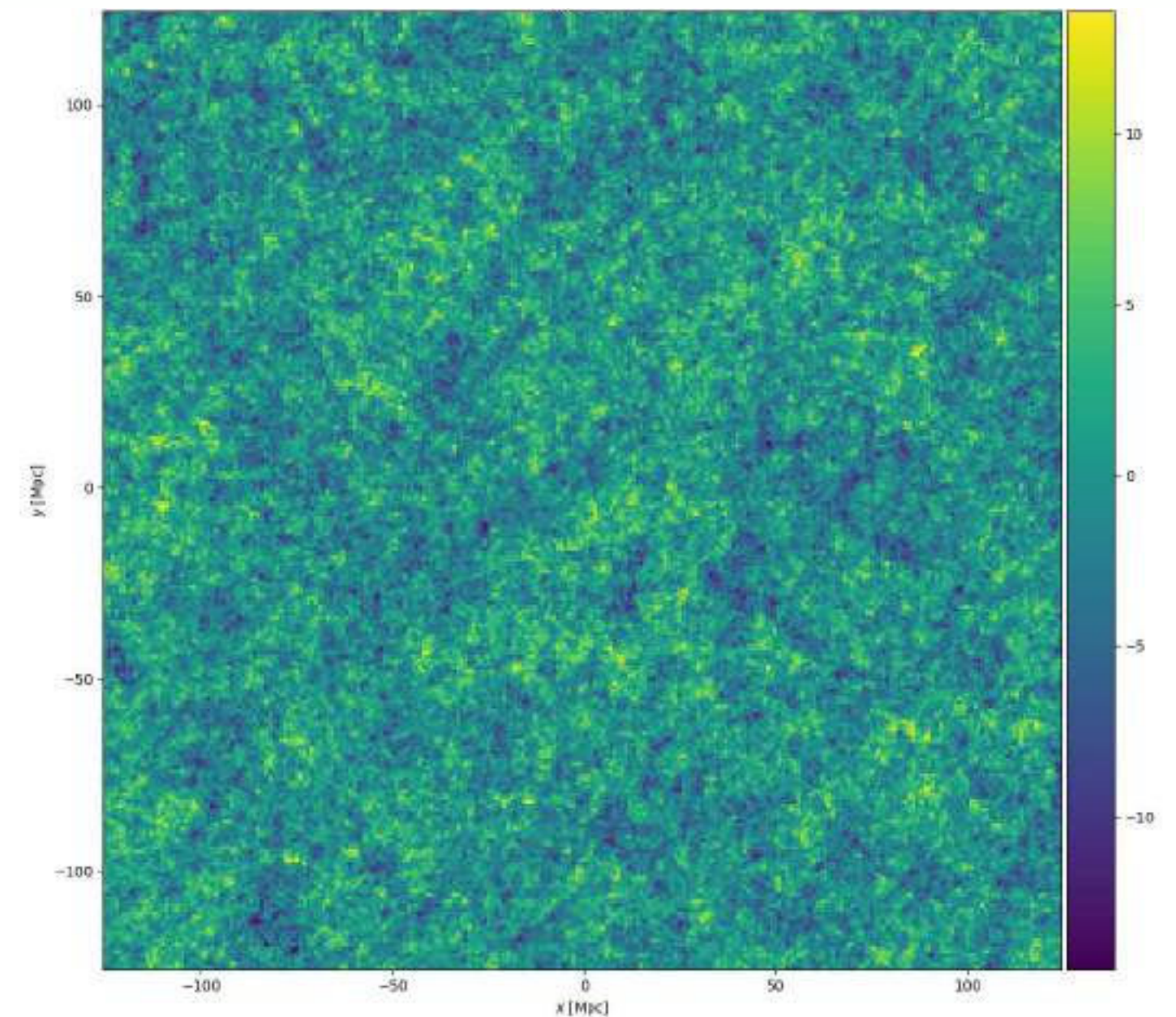
Underlying Gaussian sourced only by  $\zeta_G(\mathbf{x})$

non-Gaussian  $\delta_{nG}(\mathbf{x})$  *correlated* with  $\delta_G(\mathbf{x})$



Classical  $f_{\text{NL}}$  non-Gaussianity sourced by  $\zeta(\mathbf{x}) = \zeta_G(\mathbf{x}) + f_{\text{NL}} (\zeta_G^2(\mathbf{x}) - \langle \zeta_G^2(\mathbf{x}) \rangle)$  with  $f_{\text{NL}} = 10^5$ .

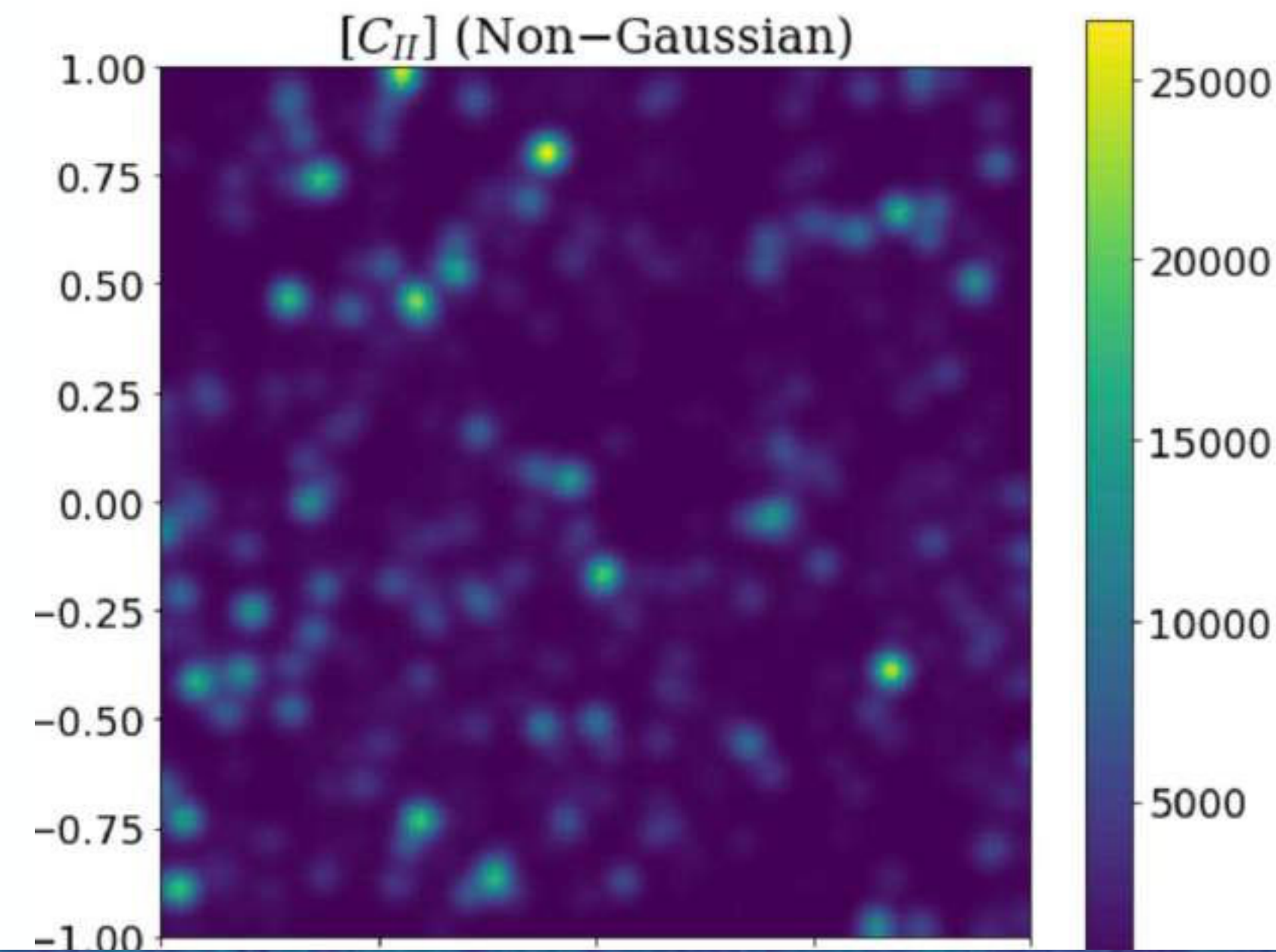
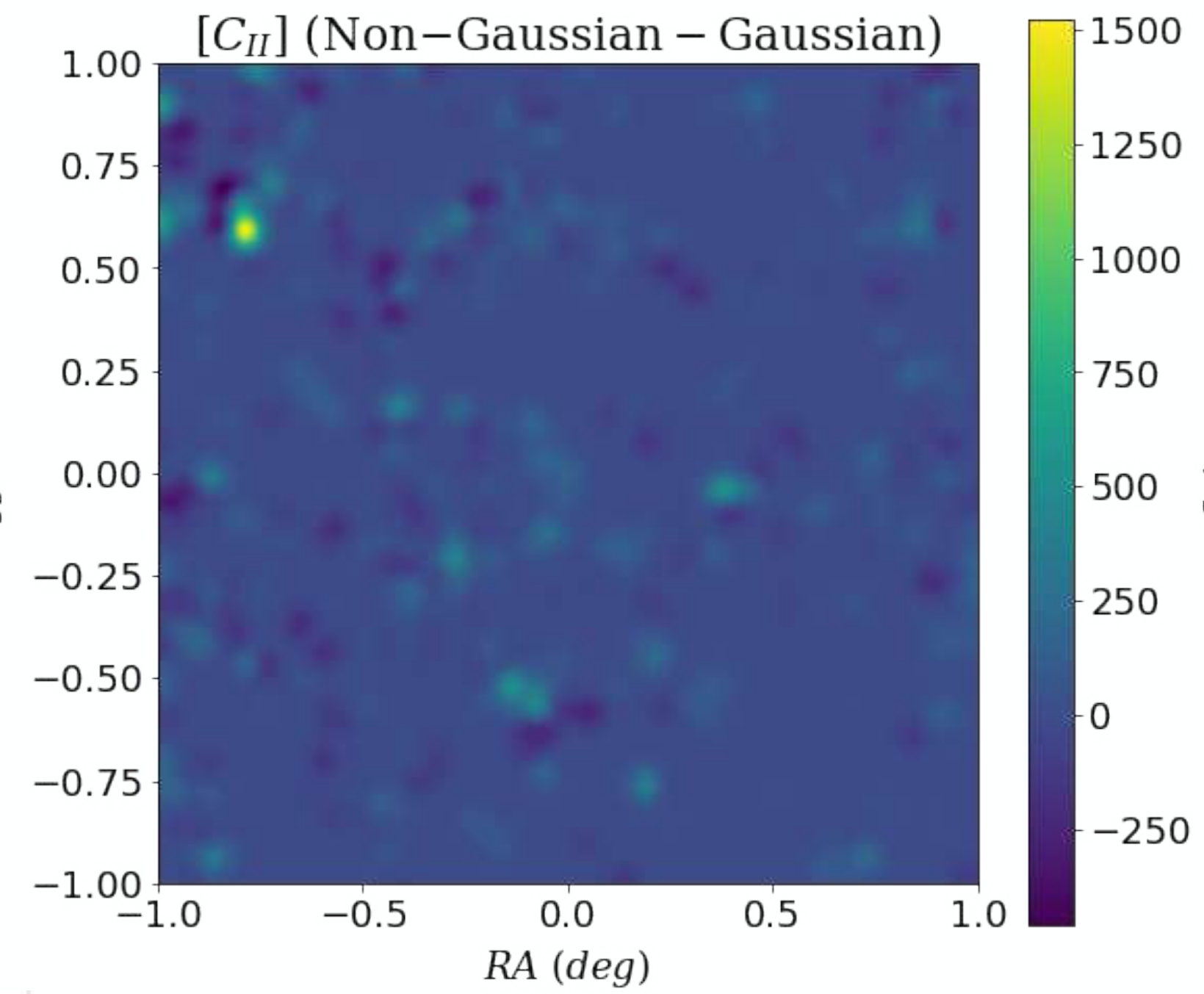
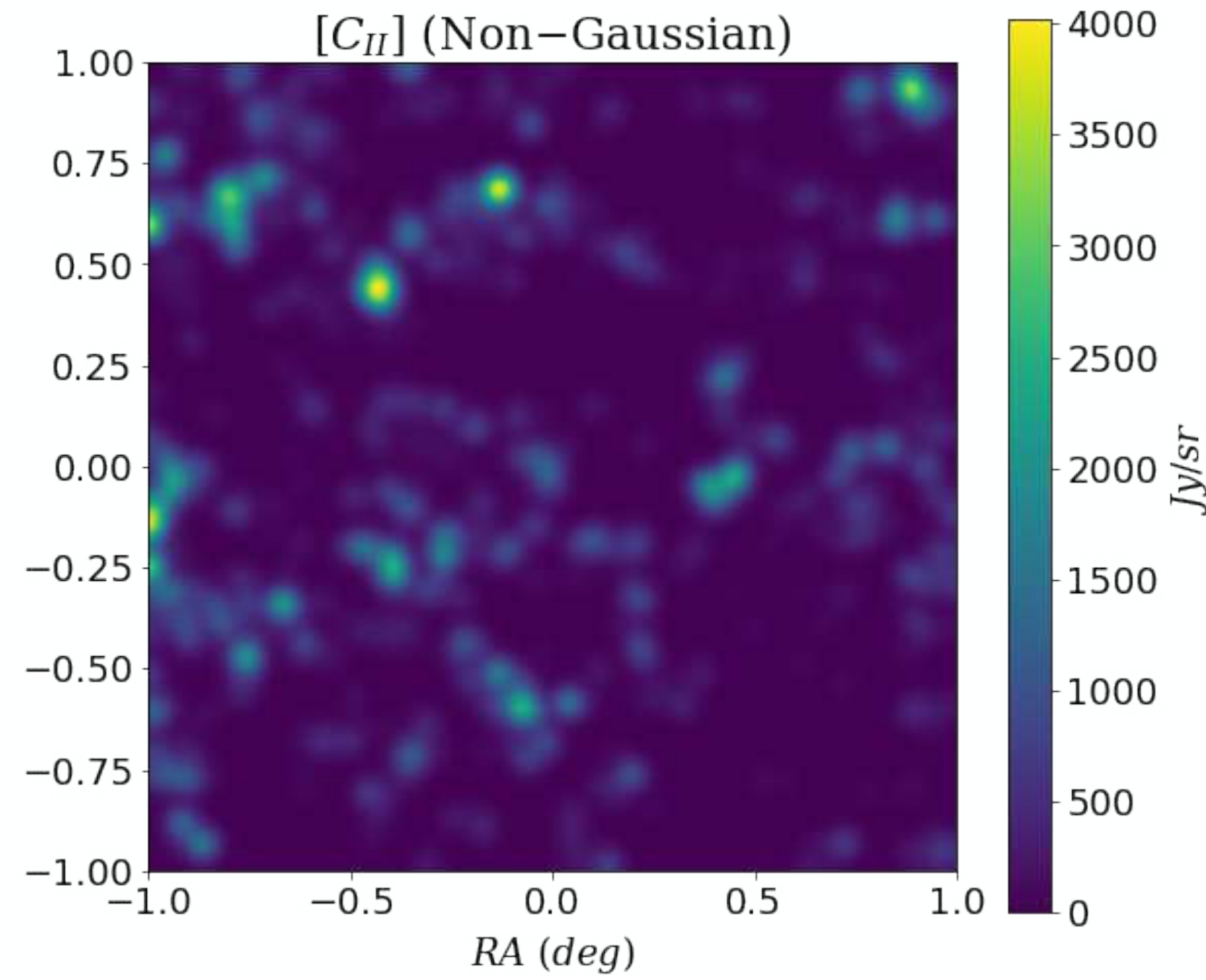
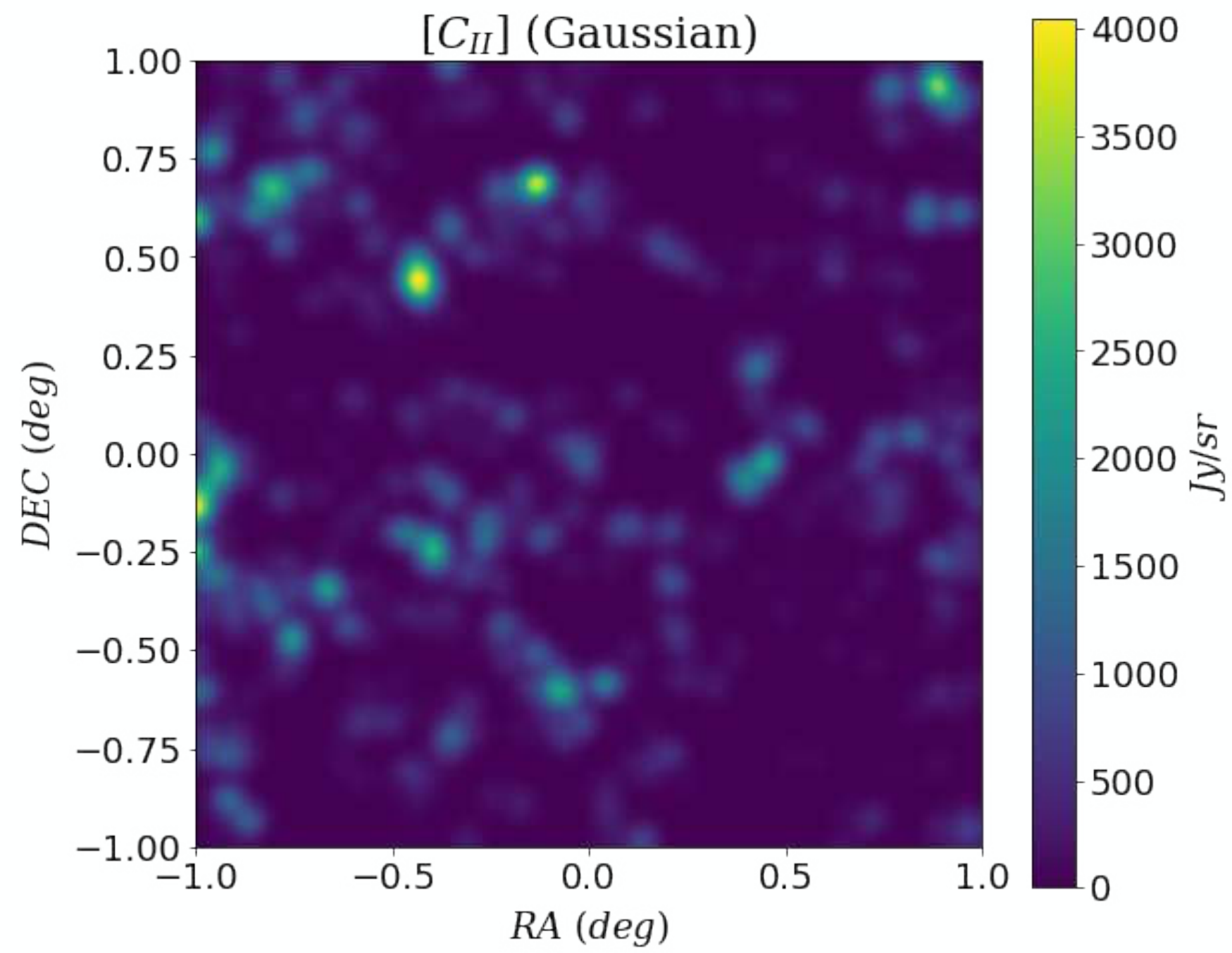
non-Gaussian  $\delta_{nG}(\mathbf{x})$  *uncorrelated* with  $\delta_G(\mathbf{x})$



Uncorrelated gaussian field  $\chi_G(\mathbf{x})$  with nearly scale-invariant power spectrum giving rise to non-Gaussianity sourced by  $\zeta(\mathbf{x}) = \zeta_G(\mathbf{x}) + \tilde{f}_{\text{NL}} (\chi_G^2(\mathbf{x}) - \langle \chi_G^2(\mathbf{x}) \rangle)$  with  $\tilde{f}_{\text{NL}} = 10^5$

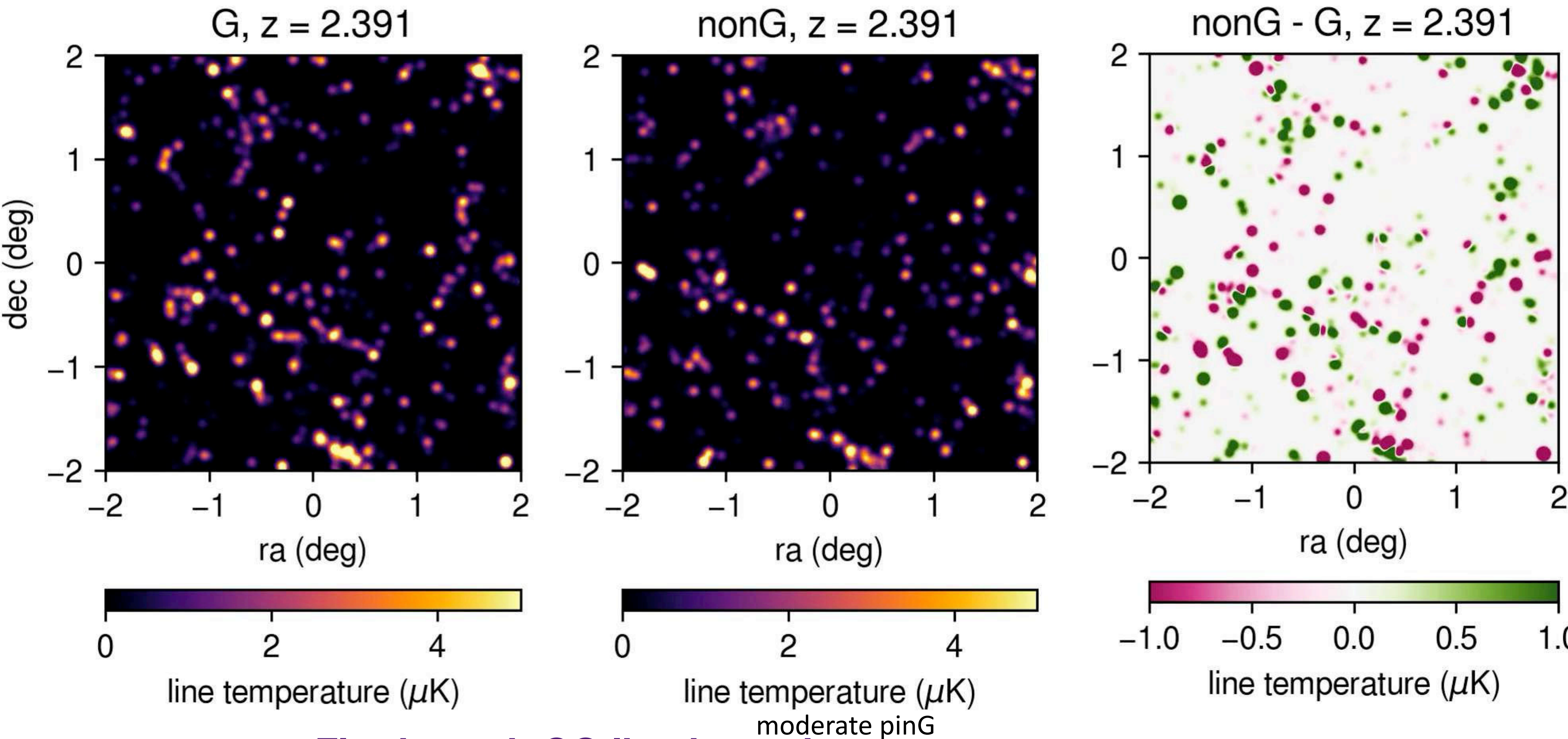


# modest instability m20



strong instability m30





## Fly-through CO line intensity maps

with and without the inflaton traversing an instability during inflation creating a pinG  
 (Bond, Carlson, Chung, Horlavage)